PEROXISOMES IN ABSORPTIVE CELLS OF MAMMALIAN SMALL INTESTINE

PHYLLIS M. NOVIKOFF and ALEX B. NOVIKOFF

From the Department of Pathology, Albert Einstein College of Medicine, Yeshiva University, Bronx, New York 10461

ABSTRACT

Huge numbers of peroxisomes are present in guinea pig duodenum, jejunum, and ileum, and in rat duodenum. The peroxisomes have been studied by light and electron microscopy, including visualization by incubation in a newly-developed alkaline 3,3′ diaminobenzidine (DAB) medium. Electron micrographs of more than 3700 guinea pig peroxisomes have been studied. The diameter of most peroxisomes ranges from 0.15 μ to 0.25 μ. They often appear in clusters, surrounded by and continuous, in numerous places, with smooth endoplasmic reticulum (ER). The ER is extremely tortuous in these regions. Serial sectioning is valuable for studying the ER-peroxisome relationships but viewing sections at different angles, tilted with a goniometer stage, is more informative. The intimate relations of the two organelles appear the same in tissue fixed in four different fixatives. The peroxisomes may be interpreted as localized dilatations of smooth ER retaining multiple membranous continuities. This interpretation is discussed in light of the turnover data on peroxisomal proteins of rat hepatocytes reported by Poole and colleagues. The very large numbers of peroxisomes in intestinal epithelium lead to speculations concerning their functional significance. They resemble the small peroxisomes described in many other cell types. Although the distinctive relationship of these peroxisomes to the ER is probably more significant than their small size, for practical purposes we propose the term "microperoxisomes" to distinguish these peroxisomes from the better-known larger peroxisomes of liver and kidney.

INTRODUCTION

In 1970 Connock and Pover (8) separated particulate fractions from homogenates of small intestine epithelium of guinea pigs treated with Triton WR-1339. One fraction showed high levels of acid phosphatase and β-glucuronidase and was considered to be rich in lysosomes. The other fraction was rich in catalase and was presumed to contain peroxisomes. Electron microscope observations on the particles were not reported; nor were data presented on the distribution of the peroxisomes in the different regions of the small intestine. The existence of particulate catalase, aryl sulfatase, and β-glucuronidase in guinea pig intestinal villi was reported in 1970 by Peters (62).

We visualized the peroxisomes by a modification, reported elsewhere[1] of the alkaline 3,3′diaminobenzidine (DAB) staining procedure of Novikoff and Goldfischer (59). The studies reported here reveal huge numbers of peroxisomes in the absorptive cells of all three parts of the guinea pig

[1] Novikoff, A. B., P. M. Novikoff, C. Davis, and N. Quintana. 1972. Facilitation of light and electron microscope study of microperoxisomes. Submitted to *J. Histochem. Cytochem.*

small intestine and in the duodenum, the only region studied, of the rat.

The peroxisomes show multiple attachments to smooth endoplasmic reticulum (ER), in a manner suggesting that they are dilated regions of ER. These smooth ER–peroxisome relations are consistent with the turnover data of Poole and colleagues on rat liver which suggest that a pool of peroxisomal proteins is readily accessible among peroxisomes, or between peroxisomes and ER (65–67). Our observations bear on the current discussions of peroxisome origin in hepatocytes (60, 15, 16, 80, 40, 84, 72, 18) and renal cells (14, 16). The abundance of peroxisomes in intestinal epithelium may have significance for the physiological roles of peroxisomes generally. The relatively uniform size and fine structure of the peroxisomes, coupled with their abundance, suggest that intestinal epithelium may be favorable material for biochemical study.

The peroxisomes of the absorptive cells resemble those found in a wide variety of other cell types. It is suggested that these peroxisomes are sufficiently distinct from the better-known peroxisomes of liver and kidney, which form the basis of the biochemical definition of peroxisomes (12), to warrant a special term. The term, microperoxisome, is proposed for the small peroxisomes, without cores, which are dilated regions of ER; multiple membranous continuities exist between these microperoxisomes and ER.

MATERIALS AND METHODS

Female albino guinea pigs, 300–700 g in weight, and female Holtzman rats, 150–200 g, were used. While the animals were etherized, three regions of the small intestine were removed and quickly immersed in fixative. Thin slices were cut and the rings were transferred to fresh fixative. Samples of duodenum came from the first 2 cm distal to the pyloric sphincter. Ileum samples were taken about 2 cm proximal to the ileocecal junction. The jejunum pieces were removed proximal to the midpoint of the small intestine. All three regions were used in the guinea pig studies; only the duodenum was studied in the rat.

The fixatives included: (*a*) cold 2.5% glutaraldehyde–0.1 M cacodylate, pH 7.4 (73) with 0.05% $CaCl_2$, 3 hr; (*b*) cold 2.5% glutaraldehyde–2% formaldehyde (prepared from paraformaldehyde)–0.09 M cacodylate, pH 7.4, with 0.025% $CaCl_2$ (46), 3 hr; (*c*) cold 1% OsO_4 in 0.1 M phosphate buffer, pH 7.4 (47), 2 hr; and (*d*) cold 1% OsO_4–2.5% glutaraldehyde, prepared according to Hirsch and Fedorko (30), 1 hr. The glutaraldehyde was purchased from Ladd Research Industries, Inc., Burlington, Vt., and the formaldehyde was freshly prepared from paraformaldehyde (Fisher Scientific Company, Springfield, N. J.).

Light Microscopy

Fixatives (*a*) and (*b*) above, and also cold formaldehyde-calcium (4) for 3 hr and overnight, were used. Frozen sections, 10 μ, cut on a Sartorius microtome were used to compare results with the Novikoff-Goldfischer DAB, pH 9.0, medium (59) and its pH 9.7 modification[1]. Three other cytochemical procedures were also performed with such sections: (*a*) acid phosphatase activity, with cytidylic acid as substrate (for ingredients of medium, see ref. [61]); and (*b*) two procedures for α-hydroxy acid oxidases, modifying the Allen-Beard method for α-hydroxy valerate oxidase (1), by substituting tetranitro-blue tetrazolium for nitro-blue tetrazolium and adding 5×10^{-3} M potassium cyanide to the medium; and the Shnitka-Talibi (76) procedure for α-hydroxy butyrate oxidase, with and without rubeanic acid posttreatment. The Graham-Karnovsky (26) procedure for urate oxidase was used on cryostat sections unfixed and postfixed for 15 min in cold acetone, cold 4% formaldehyde, or cold 1.5% glutaraldehyde. The Locke-McMahon modification (42), in which the urate concentration is drastically reduced, was also used.

As control tissues for the cytochemical procedures rat kidney was used in the two α-hydroxy oxidase procedures and rat liver in the urate oxidase procedure. It was found that both α-hydroxy oxidase procedures gave fine results after glutaraldehyde fixation, and these were used for the electron microscope cytochemistry of rat duodenum and guinea pig duodenum. For urate oxidase, postfixation of cryostat sections in acetone proved best, and this was used for light microscope examination of rat and guinea pig duodenum.

DAB cytochemistry at pH 9.0 and 9.7 was performed on all three portions of guinea pig intestine and on rat duodenum, with addition of KCN, in concentrations up to 1×10^{-2} M, or higher H_2O_2 levels up to 0.3% (higher concentrations give an over-all brown color to the sections which complicates interpretation of the preparations) or of 3-amino-1,2,4-triazole (AT) up to 2×10^{-1} M. Presoaking of frozen sections (and nonfrozen sections; see below) in AT was tried in some experiments. The AT was dissolved in the buffer used in the full medium. The sections were soaked in AT concentrations ranging from 2×10^{-2} M to 1×10^{-1} M up to 30 min, at ice temperature and room temperature. Rat liver and kidney were used as tissue controls in each of these experiments.

It was of interest to test the extent to which, if any, peroxidase contributes to the DAB staining of the intestinal peroxisomes. For this purpose observations were made on the peroxidase-rich granules of the eosinophils (2), cells which are numerous in the connective tissue surrounding the crypts. In addition, rat colon was studied because Venkatachalam et al. (81) have demonstrated an endogenous peroxidase in the ER and nuclear envelope of cells at the base of the crypts in this part of the gut. Venkatachalam et al. (81) used a short fixation (30 min) in a 2% glutaraldehyde–4% paraformaldehyde mixture in 0.15 M cacodylate buffer, pH 7.4. We therefore used this fixation as well as glutaraldehyde [fixative (*a*), above]. Guinea pig ileum was used in these experiments along with rat colon. Results of preliminary experiments led us also to dilute the glutaraldehyde-formaldehyde fixative 1:1 and 1:3 with buffer. Sections were incubated in the pH 7.6 medium of Venkatachalam et al. (81) and also in the pH 8.0, low H_2O_2 medium (which contains manganese ions) used in our laboratory for optimal demonstration of endogenous peroxidase activities in rat thyroid, submaxillary, and parotid glands (55, 56). Finally, 2,4 dichlorophenol (DCP) (found by Goldacre and Galston (23) to abolish crystalline catalase activity without affecting pea epicotyl peroxidase activity) was used with frozen sections of guinea pig ileum and rat colon, liver, and kidney. No effect on any of the DAB reactivities was observed when sections were presoaked with DCP and incubated in DAB media containing DCP, at the concentrations used by Goldacre and Galston (1×10^{-4} M), and at 8×10^{-3} M and 2×10^{-2} M DCP, concentrations used by Lucas et al. (43) and Neufeld et al. (49, 50) to assay animal tissue homogenates for peroxidase activity without interference by catalase. However, 2,6 dichlorophenolindophenol (DCPIP) (purchased from Sigma Chemical Co., St. Louis, Mo.) gave the desired results. Sections of guinea pig ileum and rat colon, liver, and kidney were incubated with 1×10^{-4} M, 4.6×10^{-3} M, and 1.2×10^{-2} M DCPIP, with and without presoaking before incubation. All DAB-incubated tissues embedded in Epon for electron microscopy were studied by light microscopy in 2 μ sections.

Further controls for the enzymatic nature of the DAB reactivity of peroxisomes, endoplasmic reticulum, and eosinophilic granules were also employed. Frozen sections of glutaraldehyde-fixed guinea pig ileum and rat colon, fixed in the formaldehyde-glutaraldehyde mixture, were treated in two ways: (*a*) they were heated for 15 min in water at 90° C and then incubated in the DAB media at the appropriate pH; and (*b*) heated and unheated sections were incubated at the appropriate DAB media which had first been exposed to UV light for 30 min to produce DAB autoxidation and filtered. The incubation times were the same as the longest times used for DAB reactivity.

Electron Microscopy

The four fixatives (*a*)-(*d*) described above ([*a*] and [*b*] followed by 1 hr of cold 1% OsO_4, cacodylate buffer, pH 7.4) were used for examination of the fine structure of the absorptive cells of guinea pig duodenum, jejunum, and ileum, and rat duodenum. The intestinal rings were cut into smaller pieces, rinsed several times in cold 7.5% sucrose for a variable length of time, and then treated with 0.5% uranyl acetate in Veronal-acetate buffer (19) for 60 min at room temperature in the dark. After dehydration in ethanols, the pieces were treated with propylene oxide and flat embedded in Epon 812 (44) so that the villi could be sectioned lengthwise. Thin sections were cut with the LKB Ultrotome using a diamond knife. They were stained in lead citrate (70) for 5 or 10 min and were observed in the Siemens Elmiskop I microscope at 80 kv.

Thin sections were also observed in the Philips 300 microscope at 60 kv. The sections were tilted by a goniometer stage, without rotation and after rotation of 83°. Micrographs were taken at 0° tilt, −10°, −20°, −30°, +10°, +20° and +30°. Seven series of such sequences were performed on guinea pig jejunum and ileum.

Consecutive serial sections of guinea pig jejunum were also studied in six instances.

For cytochemical studies, nonfrozen 20 μ sections of guinea pig duodenum, jejunum, and ileum, and rat duodenum, fixed in (*a*) or (*b*), above, were prepared on the Sorvall TC2 (Smith-Farquhar) tissue sectioner (77). They were incubated in either the DAB pH 9.0 or pH 9.7 medium containing 5% sucrose. Either KCN or AT was present in the medium in some experiments, as described above for light microscopy. Rat colon and guinea pig ileum, fixed in either glutaraldehyde or 1:1 dilution of the formaldehyde-glutaraldehyde mixture used by Venkatachalam et al. (81) (see above), were studied after incubation in either the pH 7.6 DAB medium (81) or the pH 9.7 medium, with or without DCPIP.

Rinsing in 7.5% sucrose, treatment with uranyl acetate, dehydration, and embedding were performed as described above. Thin sections were examined either unstained or stained in lead citrate for 5 or 10 min. Serial sections of guinea pig duodenum and tilted specimens of guinea pig duodenum and jejunum were also studied.

Biochemical Assays

In two separate experiments, homogenates of small intestine of guinea pigs were made in 0.25 M sucrose. Lengths of intestine were opened in

sucrose, rinsed, and removed to fresh sucrose. Epithelial and other layers were separated from the muscle by gentle scraping with a spatula. A loose suspension of tissue was diluted with four times the volume of sucrose and briefly homogenized in a Potter-Elvejehm type homogenizer. Centrifugation in an angle-head high-speed attachment of the International refrigerated centrifuge at 600 *g* for 10 min removed erythrocytes, unbroken epithelial cells, nuclei, and large cell membrane fragments. The cytoplasmic extracts were assayed for urate oxidase activity by Dr. Harold Strecker, Department of Biochemistry, in the presence of 0.1% Triton X100 as described by Leighton et al. (41).

RESULTS

Guinea Pig Small Intestine

CYTOCHEMICAL AND RELATED OBSERVATIONS: Light microscope examination of frozen sections (10 μ) of DAB-incubated material and "thick" sections (1–3 μ) of incubated material embedded in Epon yields similar results. The villus core and the connective tissue surrounding crypts and glands contain the most deeply-stained structures: erythrocytes and eosinophil granules (Fig. 2). In the absorptive cells, there are innumerable dotlike peroxisomes (Figs. 1–3). Duodenal cells possess spherical bodies filled with electron-opaque grains; these are also DAB-positive. However, most of these can readily be distinguished from peroxisomes; they are considerably larger (Fig. 1).

No difference in size or number of peroxisomes is apparent in the three regions of small intestine. Numerous peroxisomes are present in the basal portions of the cells but the organelles are most concentrated in the apical cytoplasm (Fig. 3).

Electron microscopy, similarly, reveals no differences either in size or number of peroxisomes among duodenum, jejunum, and ileum. More than 3700 peroxisomes were counted in the electron micrographs taken of the absorptive cells.

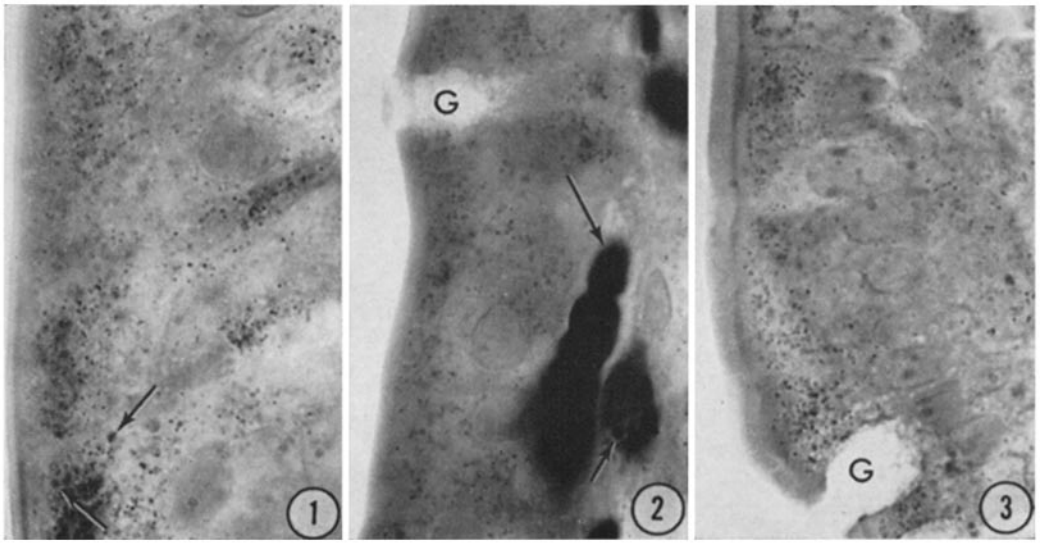

FIGURES 1–3 Light micrographs of portions of villi in Epon sections, about 2 μ thick, of guinea pig intestine. Fixed in glutaraldehyde. Incubated in DAB, pH 9.7, for 120 min. Photographed, with green filter, under oil immersion. × 1000.

FIGURE 1 Duodenum. Except for the larger granules (arrows) at bottom left, which electron microscopy shows to contain electron-opaque grains, the stained granules in the absorptive cells are peroxisomes. The striated border (at left) and the nuclei are barely evident.

FIGURE 2 Jejunum. Numerous peroxisomes are seen in the absorptive cells. The large deeply stained structures are erythrocytes (long arrow) and granules within an eosinophil (short arrow). A goblet cell is seen at *G*. The nuclei are barely evident.

FIGURE 3 Ileum. Numerous peroxisomes are seen in the absorptive cells. A goblet cell is seen at *G*. The nuclei are barely evident.

Of these, about 2100 are in sections incubated in alkaline DAB media.

Electron microscopy confirms the presence of peroxisomes throughout the cytoplasm, with the highest concentration in the supranuclear cytoplasm, excluding the terminal web and some distance below it. Peroxisomes are not found near the terminal web, where mitochondria and multivesicular bodies are numerous (Fig. 4). A single peroxisome has been observed close to the terminal web. The large numbers of peroxisomes are strikingly revealed in low magnifications of DAB-incubated material (Fig. 4). In addition to the light micrographs and low magnification electron micrographs, other figures emphasize the abundance of peroxisomes.

Many peroxisomes are found in clusters, as seen in individual sections and made even more apparent in serial sections. The most concentrated cluster (not illustrated) had twelve peroxisomes within an area of 1.2 μ^2.

Many peroxisomes are elongate (see especially Figs. 7, 10, 13, 22–24, and 33). When sectioned transversely or tangentially, such elongate forms would show circular profiles. However, roughly spherical peroxisomes are also abundant, as demonstrated by serial sections. About 70% of circular profiles have diameters ranging from 0.15 μ to 0.25 μ. About 15% are below this range, down to 0.075 μ; some are undoubtedly tangential sections of larger ones. About 15% have larger diameters, extending to 0.4 μ. An element of subjectivity enters measurements of elongate profiles. Many show constrictions and it may be reasonable to consider them as two peroxisomes connected to each other (Figs. 4, 5, 7, 12, and 13) or even as three connected peroxisomes in some instances. In view of the widespread continuities with ER, described in the next section, it is academic to debate whether the elongate forms which show no necks (Figs. 5, 13, and 33) may soon become constricted. Lengths of such elongate forms range from 0.25 μ to 0.80 μ. Cradle-like forms, such as in Figs. 24 and 28, are probably curled peroxisomes viewed from different directions.

When consideration is taken of the small size of the average peroxisome, near the limit of resolution of the light microscope, and the clustered distribution of these organelles, it is likely that many of the apparent peroxisomes in light micrographs of DAB-incubated sections are composites rather than individual organelles.

Fig. 9 illustrates the absence of acid phosphatase activity in peroxisomes of guinea pig duodenum mucosa. The same is true in the mucosal cells of guinea pig jejunum and ileum, and of rat duodenum[2].

Consistent with the absence of inner nucleoids or cores (see below), biochemical assay of cytoplasmic fractions of small intestine from two different guinea pigs shows no urate oxidase activity, measured biochemically[3]. (No inhibitor of urate

[2] It should be noted that a great many macrophages are found in the villus cores. These cells possess large lysosomes with high levels of acid hydrolase activities. These would greatly complicate biochemical assays of lysosomal activities of intestine. Separated mucosal cells would be needed for meaningful data on the epithelial cells. In contrast, the villus macrophages show only occasional small circular regions staining with DAB at pH 7.6, 8.0, 9.0, and 9.7.

[3] After submitting this manuscript, we learned that T. J. Peters in 1970 had reported the absence of urate oxidase in homogenates of guinea pig intestinal villi (62).

FIGURE 4 Guinea pig ileum. Fixed in glutaraldehyde. Incubated in DAB, pH 9.7, for 100 min. Numerous electron-opaque peroxisomes are evident. Their proximity to endoplasmic reticulum (*ER*) is discernible even at this low magnification. Arrows indicate peroxisomes which may be considered as elongate or as two peroxisomes in continuity. A multivesicular body (*MVB*) and other lysosomes (*L*) show no reaction product. Also evident in the figure are the microvilli projecting into the lumen (*LU*), mitochondria (*M*), intercellular spaces (*IS*), and desmosomes (*D*), all without reaction product. × 8800.

FIGURE 5 Guinea pig duodenum. Fixed in glutaraldehyde. Incubated in DAB medium, pH 9.0, for 120 min. Note the intercellular spaces (*IS*) separating the portions of three cells in the figure. A cluster of peroxisomes is indicated by the long arrow; note that the endoplasmic reticulum (*ER*) near it is smooth. Ribosomes (*R*) are seen elsewhere. The short arrow indicates an elongate peroxisome with a partial constriction. A multivesicular body (*MVB*) is free of reaction product. The mitochondrion below *M* is dense, not because of DAB reaction product, but because it is in the "condensed form"; compare with the "orthodox" mitochondrion above it. × 10,000.

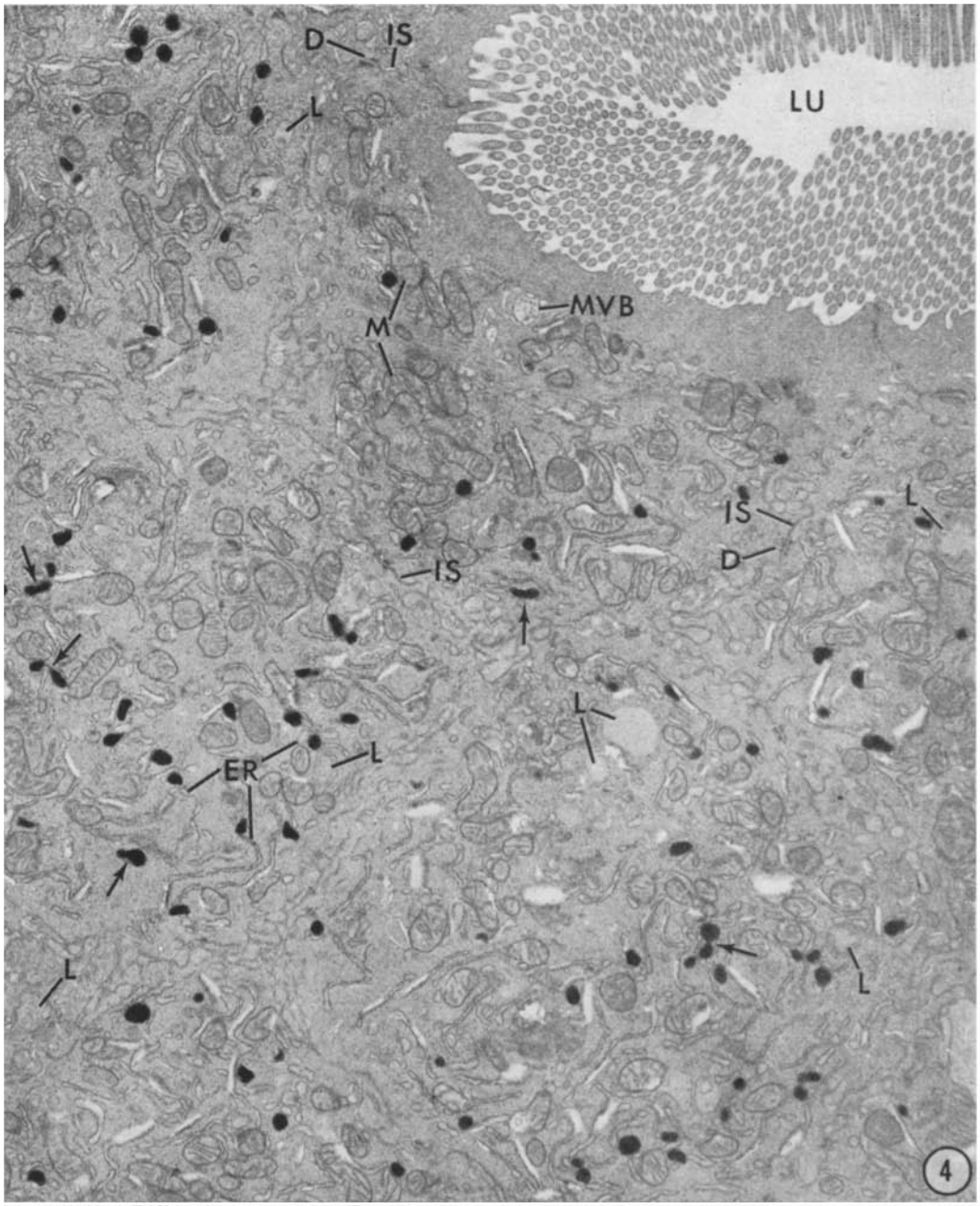
D
IS
L
LU
MVB
M
IS
L
IS
D
IS
L
ER
L
L
L
4

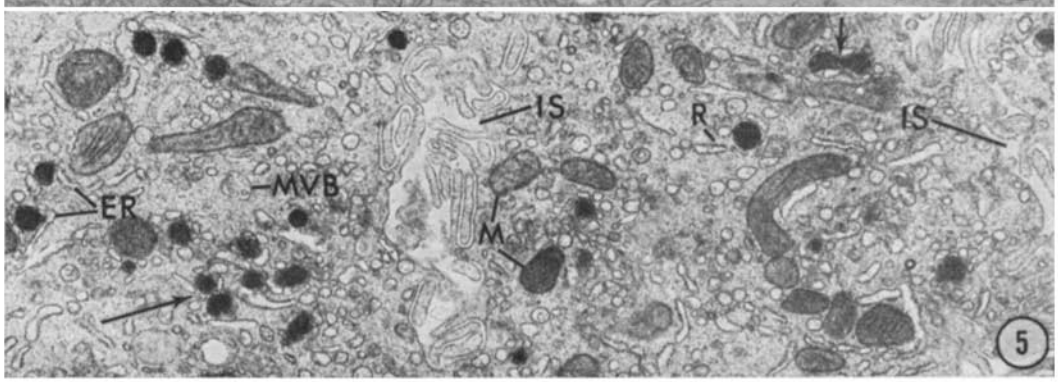
IS
R
IS
ER
MVB
M
5

oxidase activity is present in these fractions, as tested by addition to mouse liver homogenates.) Sections of guinea pig intestine show no staining by the Graham-Karnovsky procedure for urate oxidase[4].

Neither light microscopy nor electron microscopy reveals α-OH butyric acid oxidase in glutaraldehyde-fixed guinea pig duodenum after incubation in the Shnitka-Talibi medium. The electron microscope experiments should be regarded as preliminary. Frozen sections of glutaraldehyde-fixed rat kidney showed fine localization of this oxidase at the light microscope level. In contrast, we have thus far been unsuccessful in demonstrating such oxidase activity in nonfrozen sections of glutaraldehyde-fixed rat kidney used for electron microscopy.

[4] Negative results with this procedure, even on a tissue level, need to be interpreted cautiously. Sections are cut from unfixed frozen tissue and are then fixed in cold acetone. High levels of urate oxidase activity probably need to remain in sections for a positive reaction. The reliability of this method on the intracellular level is questionable.

The peroxisomes react more strongly with DAB at pH 9.7 than at pH 9.0 (cf. Fig. 8 with Fig. 6). They react only lightly in the pH 7.6 medium of Venkatachalam et al. (81).

As is generally true of peroxisomes (59, 29, 17, 7, 64, 20, 21, 82, 68), the alkaline DAB reactivity of the organelles in the absorptive cells is inhibited by AT. Often, the inhibition of peroxisomal staining is total (Fig. 7) but sometimes it is only partial. This is true even when sections are presoaked and incubated in AT concentrations as high as 1×10^{-1} M [5]. Peroxisomal staining at pH 9.0 or 9.7 is unaffected by KCN, even at 1×10^{-2} M with presoaking. By light microscopy, the lowest DCPIP concentration used (1×10^{-4} M) completely abolishes peroxisome reactivity, even without presoaking. This is true of electron microscopy at 4.6×10^{-3} M and 1.2×10^{-2} M DCPIP, and at 1×10^{-4} M for virtually all cells

[5] We have not established the factors responsible for the variability in response to AT. This variability was paralleled in rat liver and kidney, used as control tissues each time the small intestine was studied.

FIGURE 6 Guinea pig duodenum. Fixed in glutaraldehyde. Incubated in DAB medium, pH 9.0, for 100 min. The endoplasmic reticulum (ER) is devoid of ribosomes, as is all of the cytoplasm in the micrograph. Note the tortuosity of the ER surrounding peroxisomes No. 1– No. 4 and below No. 5. The tortuous delimiting membrane of No. 1 is seen clearly only in areas. Peroxisome No. 1 may represent an early stage of SER dilatation to form a peroxisome; the short arrow indicates irregular electron-opaque structures. The delimiting membranes of No. 4 and No. 5 are clearly seen except where the peroxisomes are probably continuous with the tortuous SER. Note, at the long arrow, a series of strands between the peroxisome No. 5 and the ER. × 81,000.

FIGURE 7 Guinea pig duodenum. Fixed in glutaraldehyde. Presoaked in 2×10^{-2} M AT at pH 9.7 for 30 min in the cold, and incubated in DAB medium, pH 9.7, containing 2×10^{-2} M AT for 100 min. Complete inhibition of the DAB reaction is evident. Note that the endoplasmic reticulum (ER) alongside the seven peroxisomes is devoid of ribosomes; the same is true of the surrounding cytoplasm. Peroxisomes No. 1 and No. 3 appear as dilatations of the ER; note inner circular profiles at arrows. Tubule-like inner strands may be seen in No. 4– No. 6. The continuity beween No. 2 and No. 3 is evident except in a small area. The continuity of SER and No. 6 is indicated by an arrowhead. Note at the upper surface of No. 7 the linear strands below the delimiting membrane; cf. No. 5 in Fig. 6 where the strands are also seen external to the peroxisome. × 79,000.

FIGURE 8 Guinea pig ileum. Fixed in glutaraldehyde. Incubated in DAB medium, pH 9.7, for 100 min. A few ribosomes (*R*) are evident on the ER, but the peroxisomes are surrounded by SER. Arrowheads indicate continuities between the peroxisome membranes and SER. Internal strands between the inner portion of the peroxisome and the delimiting membrane are seen in No. 1, to the right. Dark undulating structures may be seen within No. 2 and No. 4. × 81,000.

FIGURE 9 Guinea pig duodenum. Fixed in glutaraldehyde-formaldehyde. Incubated for acid phosphatase activity, with CMP as substrate, for 30 min. Two lysosomes (*L*), probably autophagic vacuoles, are strongly positive but neither peroxisomes (*P*) nor mitochondria (*M*) show reaction product. Note ribosomes (*R*) on the endoplasmic reticulum (ER) and apparently free in the cytoplasm. × 33,000.

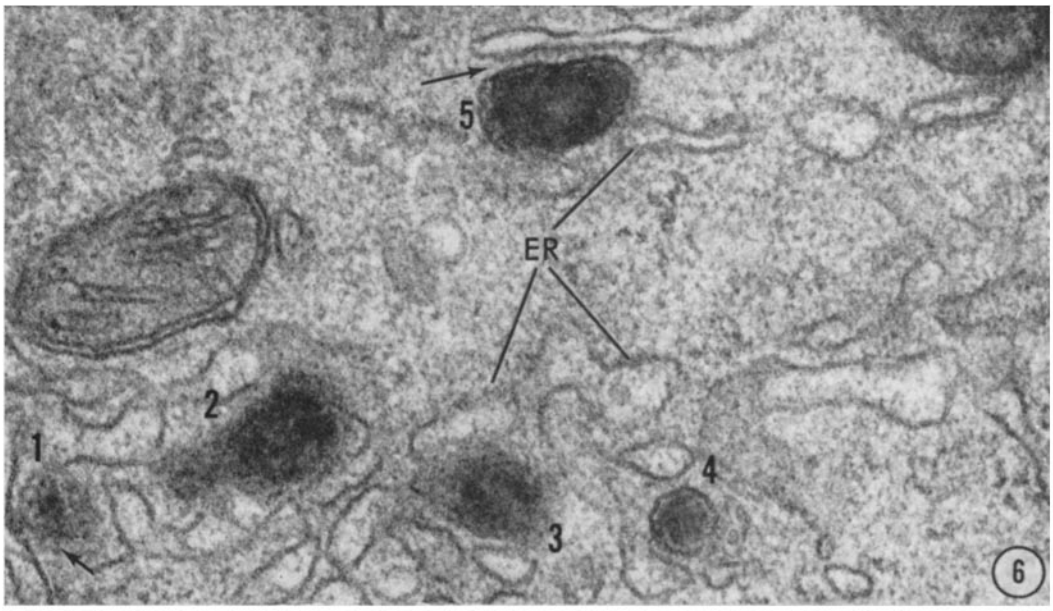
5
ER
2
1
4
3
6

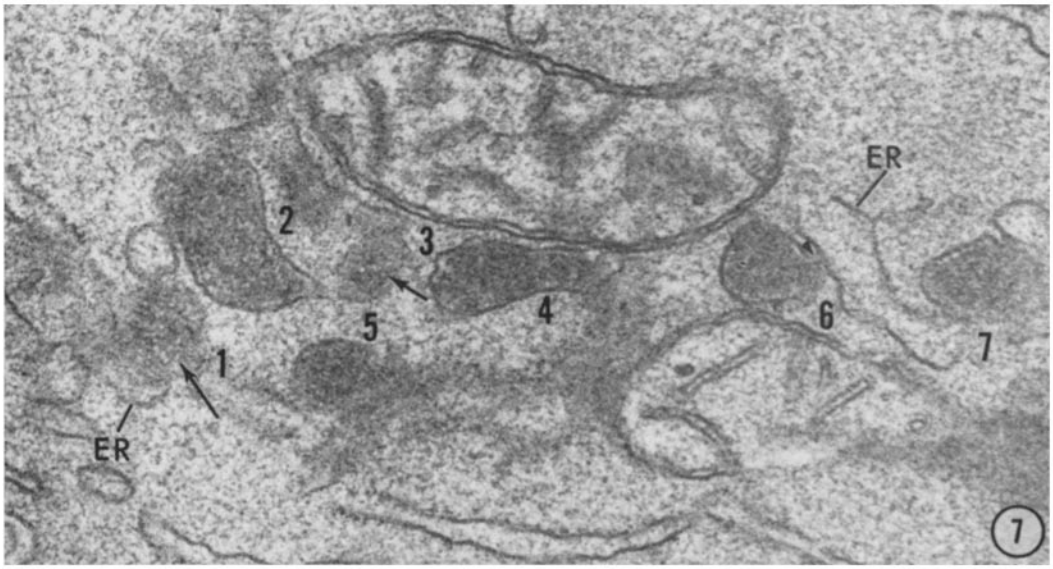
ER
2
3
5
4
6
7
1
ER
7

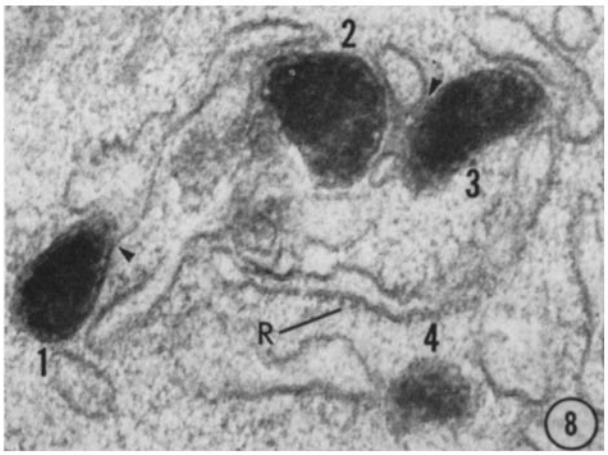
2
3
1
R
4
8

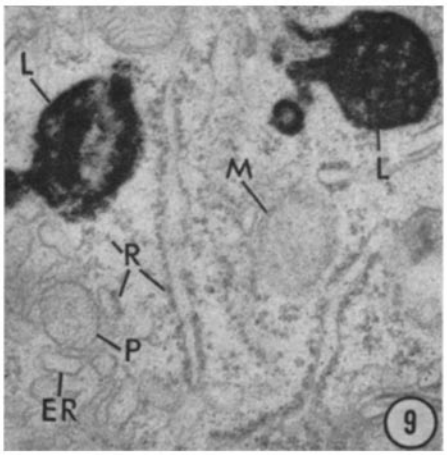
L
M
L
R
P
ER
9

(Fig. 11)[6]. A rare cell may show slight DAB reactivity at 1×10^{-4} M DCPIP when the nonfrozen sections are not presoaked. In contrast, DCPIP has no effect upon the reactivity at pH 7.6 in the crypt cells of rat colon and little, if any, upon the eosinophil granule reactivity at either pH 7.6 or 9.7. The highest level of H_2O_2 used did not diminish the staining of the peroxisomes.

Guinea pig ileum shows no ER or nuclear envelope reactivity under any conditions tried, including incubation of formaldehyde-glutaraldehyde fixed tissue in the pH 7.6 and pH 8.0 media, which give strong ER staining in the crypt cells of rat colon. Judged by light microscopy, the pH 8.0, low H_2O_2 medium is more optimal for such ER staining than the pH 7.6 medium used by Venkatachalam et al. (81). Glutaraldehyde fixation [fixative (*a*)] strongly inhibits the ER staining. However, by prolonging the incubation time (beyond 90 min) ER staining may be shown in such material; this yields better fine structure preservation than the short Venkatachalam et al. fixation. When the full glutaraldehyde-formaldehyde mixture (81) was used, light microscope visualization of the ER was hindered because of mitochondrial staining. However, diluting the fixative 1:1 or 1:4 with buffer gave results like those in Fig. 1 of Venkatachalam et al. (81). The 1:1 diluted fixative was used for electron microscope study of both guinea pig ileum and rat colon. Electron microscopy confirms the light microscope observations; ER staining does not occur in guinea pig ileum. In contrast, ER and nuclear envelope of crypt cells of rat colon stain strongly in the pH 7.6 DAB medium. Staining occurs even in the pH 9.7 DAB medium, but it is much diminished, too little to be seen by light microscopy (in both Epon sections and frozen sections) and barely sufficient for electron microscopy.

Rat ileum peroxisomes are not visualized by light or electron microscopy in the 7.6 medium, even after 200 min of incubation.

Preheating frozen sections for 15 min at 90° C completely inhibits peroxisomal staining in guinea pig ileum after 200 min of incubation in the pH 9.7 medium, as viewed by light microscopy. The staining of ER at pH 7.6 in the crypt cells of rat colon is also inhibited, as is the staining of eosinophil granules at both pH 7.6 and 9.7. Erythrocytes stain slightly at the lower pH and more strongly (although much below control levels) in the pH 9.7 medium with its high H_2O_2 level. No evidence of adsorption of preoxidized DAB by any cell component is seen under the conditions of incubation which we employed.

PEROXISOME RELATIONSHIPS TO ER AND RIBOSOMES: The most interesting aspect of the present study of intestinal cells is the intimate and complex relationship of their peroxisomes to the ER. The vast majority of the peroxisomes are found in regions of *smooth* ER which run parallel to or surround the peroxisomes. Generally, ribosomes are not seen in the areas where the peroxisomes are clustered (Figs. 6–8, 10–13, and 25–33). Sometimes, unidentified spicule-like structures, perhaps portions of ribosomes or points of earlier ribosome attachment, are seen on the ER (Figs. 8, 20, and 32).

It is quite rare to find ribosomes on the ER membranes (i.e., rough ER) close to the region of membrane continuities between ER and peroxisomes. Indeed, rough ER near peroxisomes required deliberate search. It is to be stressed, therefore, that a strong bias exists in favor of rough ER in selecting the illustrations (Figs. 9, 14, 15, 19, and 21). The chief reasons for such selection are: (*a*) our desire to demonstrate that preparative steps such as fixation (Figs. 9, 14, 15, 16, and 19) and incubation with DAB (Figs. 5, 8, 21, 29, and 30) are not responsible for the failure to see ribosomes in the peroxisomal areas; when present, the ribosomes are readily visible in the micrographs; (*b*) to permit the unequivocal assertion that the smooth membranes in continuity with the peroxisomes are indeed smooth ER since its continuity with rough ER is documented (Figs. 14, 15, and 19); and (*c*) there are claims in the literature, from DAB staining observations, that in hepatocytes catalase is synthesized at the ribosomes and goes directly to the peroxisomes without transit through the ER.

Not once in the electron micrographs of DAB-incubated sections, which include about 2100 peroxisomes, does a ribosome show DAB reactivity, whether it is ER-bound or free, near the peroxisomes or not.

It should be noted that in all regards described above, as with other fine structure features to be considered below, all four fixatives yield the same

[6] Rat kidney peroxisomes are consistently, but not completely inhibited. Rat liver peroxisomes appear to be inhibited in nonfrozen sections but not in frozen sections. Further study of these results is in progress.

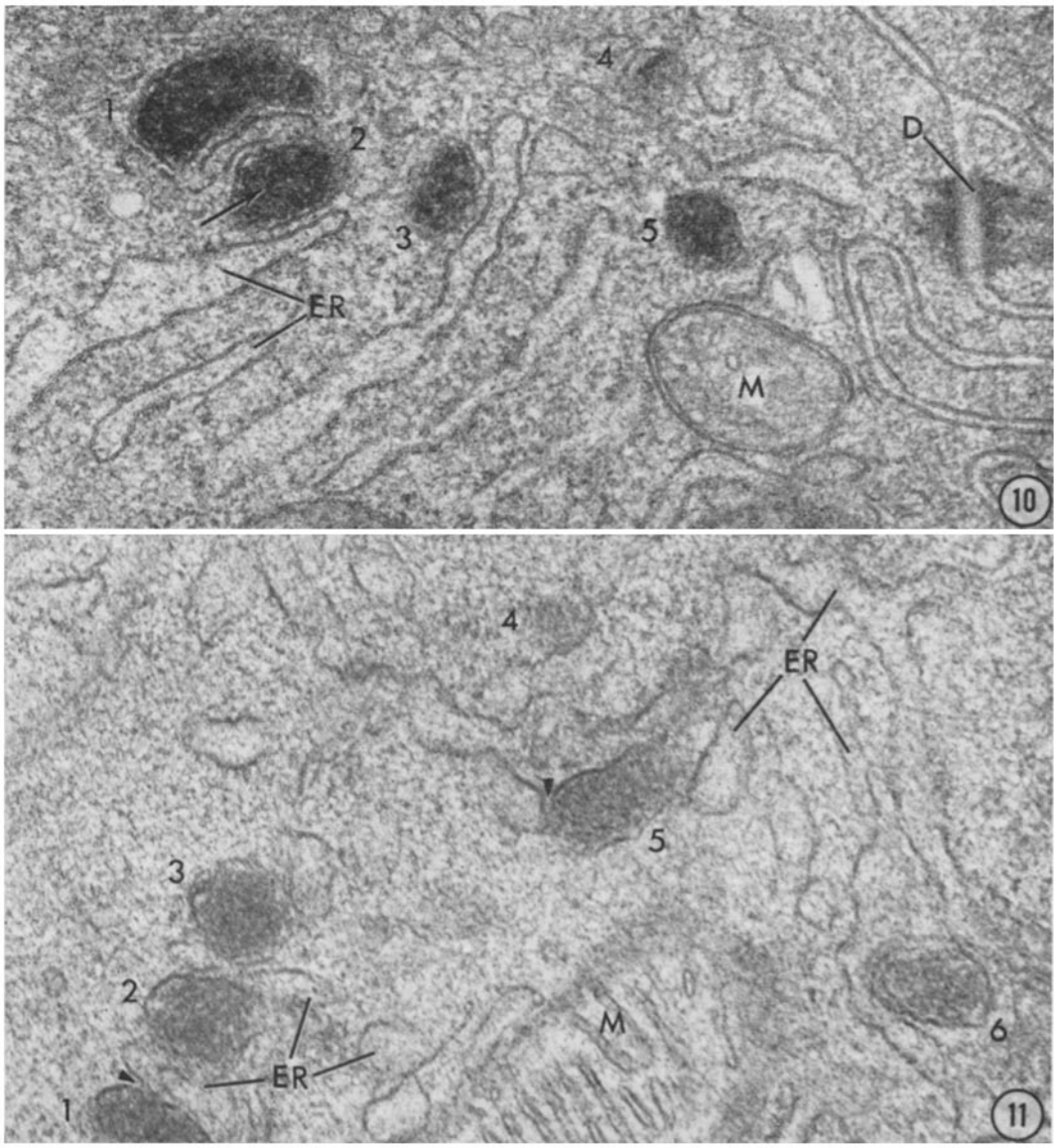

FIGURE 10 Guinea pig ileum. Fixed in glutaraldehyde. Incubated in DAB, pH 9.7, for 90 min. Nonfrozen section presoaked in buffer, pH 9.7, for 60 min at 4°C. The tripartite nature of peroxisomal membranes and SER (*ER*) is well visualized. Note the tortuosity of the delimiting membrane of peroxisome No. 2. Reaction product is restricted to the peroxisomes, numbered 1–5; none is present in endoplasmic reticulum (ER), mitochondria (*M*), or desmosomes (*D*). Arrow indicates tubular structures within peroxisome No. 2. × 64,000.

FIGURE 11 Guinea pig ileum. Fixed in glutaraldehyde. Incubated for 180 min in DAB, pH 9.7, containing 1×10^{-4} M DCPIP. Nonfrozen section not presoaked. All peroxisomes show complete inhibition of DAB reactivity. Note the undulating nature of the SER (*ER*). Arrowheads indicate continuities of peroxisomes and SER. A grazing section of a mitochondrion is seen at *M*. *ER*, endoplasmic reticulum. × 64,000.

results. Similarly, DAB-incubation results are the same whether tissue is fixed in glutaraldehyde or in the glutaraldehyde-formaldehyde mixture. Incubation of tissue in the DAB medium does not alter ultrastructural relationships, but fine irregular structures within the peroxisomes are more apparent after DAB incubation.

TORTUOSITIES AND DILATATIONS OF THE ER: In the areas containing peroxisomes, the only regions which we studied, the smooth ER is tortuous or undulating (see particularly Figs. 6, 8, 11, 27, and 33). This contributes to the frequent inability to discern, in individual sections, both the tripartite nature of ER and the continuities that exist between ER and peroxisomal membranes, which are also tortuous (Figs. 10, 11, 15, 28, and 33). The tripartite nature of the peroxisome membrane is evident in Figs. 6, 7, 10, 23, 24, and 33. Obviously, the illustrations are highly selected to show ER-peroxisome continuities (Figs. 8, 11, 16, 19–21, 23, 24, 28, and 33). Yet, even among these micrographs such continuities often disappear in areas, or are blurred in regions. Nevertheless, the tripartite membrane is continuous in both ER and its dilatations, the peroxisomes. This is more readily appreciated when sections are examined from different angles, tilted by the goniometer stage (Figs. 31, 32, and 33). Apparent breaks in the membrane disappear when the section is properly tilted.

Figs. 25, 26, 29, and 30 show two sets of serial sections. They were selected because continuity of SER and some peroxisomes is evident. In other serials, even fewer peroxisomes show the multiple continuities that probably exist.

On the other hand, of 56 peroxisomes examined at random in tilted sections, every single one shows multiple continuities to the ER. Only a few of these continuities can be illustrated (Figs. 27, 28, and 31–33).

Images are frequently encountered that may represent early stages of ER dilatation to form peroxisomes (Figs. 6, 7, 17, 18, and 20). Unlike the fully-condensed peroxisomes there is a fairly wide electron-lucent area between the inner material and ER membrane.

What has been referred to as the continuity of one peroxisome with another, here and in the literature, may as well be described as multiple, unseparated, dilatations of ER. Such areas are seen in Figs. 4, 5, 7, 12, 13, and 25.

INNER STRUCTURE OF PEROXISOMES: Nucleoids or corelike structures are not observed in the peroxisomes of the absorptive cells, irrespective of the fixative used. Except in one sample of duodenum fixed in glutaraldehyde-formaldehyde (Fig. 16), the interior of the organelles is distinctly heterogeneous. Higher resolution studies will be required to describe the inner structure of the peroxisomes more adequately. They appear as irregularly arranged, tubule-like structures

FIGURE 12 Guinea pig jejunum. Fixed in OsO_4-phosphate. Note the absence of ribosomes on the ER or in the cytoplasm. In peroxisome No. 1 the upper arrow indicates a wavy structure; the lower arrow is directed towards a tubule-like structure. A wavy tubule-like profile is seen within No. 5 (arrow). Note the continuity of No. 3 and No. 4. Continuities of peroxisomal membranes and ER are indicated by arrowheads. × 41,000.

FIGURE 13 Guinea pig jejunum. Fixed in OsO_4–phosphate. No ribosomes are seen, either on the ER or in the cytoplasm. Short arrows indicate circular and linear profiles within peroxisome No. 1 and No. 5. Arrowheads indicate continuities of SER with peroxisomes. A long arrow indicates an hourglass-like constriction between No. 4 and No. 5. × 43,000.

FIGURE 14 Guinea pig duodenum. Fixed in OsO_4–glutaraldehyde. Note the presence of ribosomes (*R*), both on the ER and apparently free in the cytoplasm. However, the ER related to the seven peroxisomes is devoid of ribosomes. Continuities of peroxisome membranes and SER are indicated by arrowheads. Arrows indicate wavy tubule-like structures in No. 4 and No. 5. × 47,000.

FIGURE 15 Guinea pig duodenum. Fixed in OsO_4–glutaraldehyde. Arrays of roughly parallel RER are common in the absorptive cells but it is rare to find peroxisomes in these arrays, such as in this figure. Ribosomes (*R*) are unusually close to peroxisomes in this field, but note that it is SER with which the two peroxisomes are connected (arrowheads). The continuity of SER with RER may be seen near both peroxisomes. Free ribosomes (*R*) are seen to the left of the lower peroxisome. The two arrows indicate tubule-like structures within the peroxisomes. × 54,000.

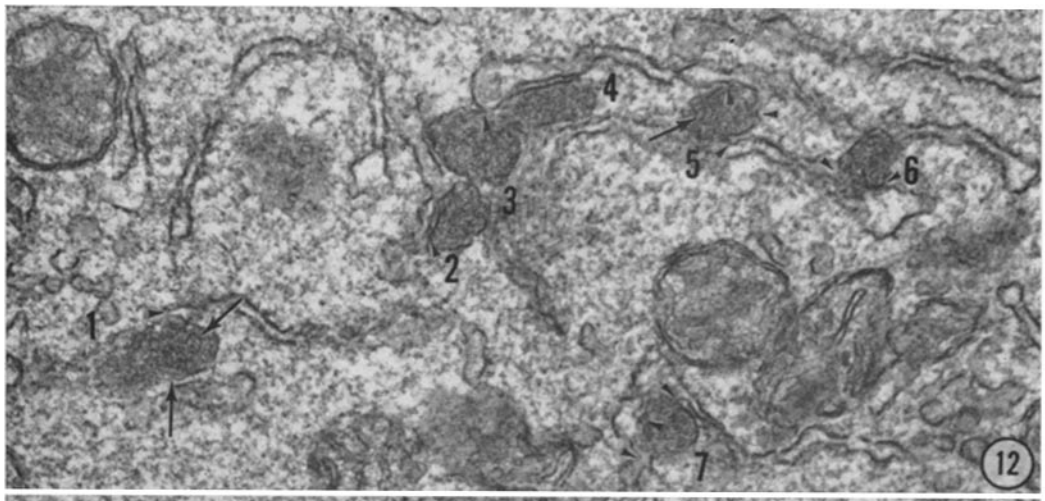
1
2
3
4
5
6
7
12

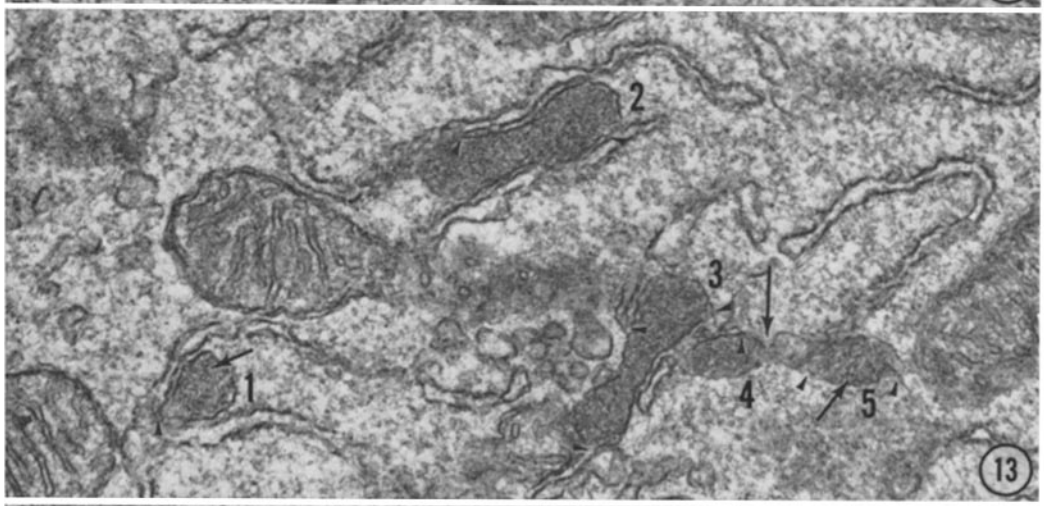
1
2
3
4
5
13

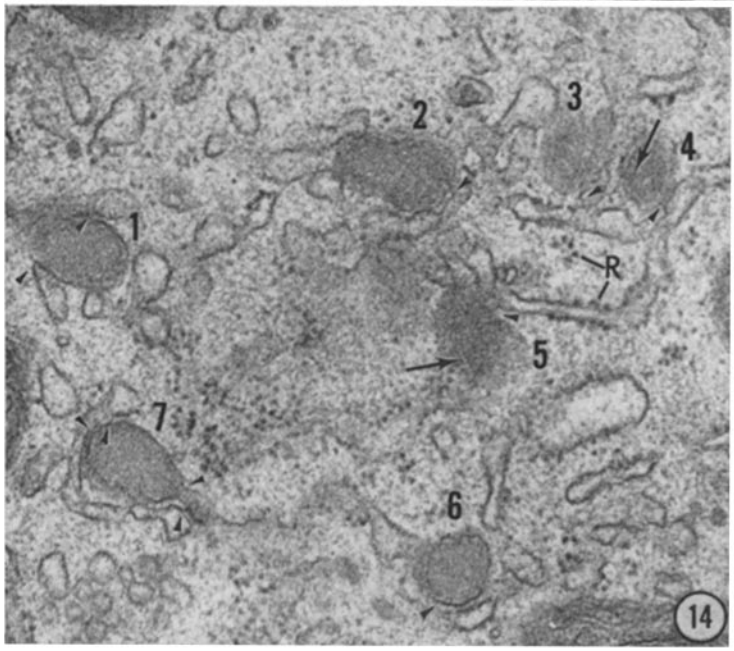
1
2
3
4
5
6
7
R
14

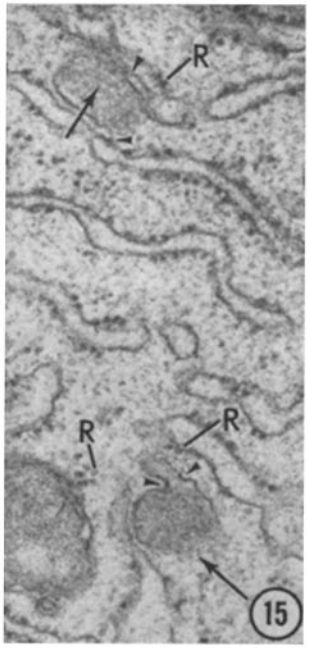
R
R
R
15

(Figs. 10, 12–15, 19, 27, 28, and 33). Transverse sections would be seen as circular profiles. These are often observed (Figs. 7, 11, 13, 17, 21, and 27–33). After incubation in the alkaline DAB medium, rather irregular strands are seen (Figs. 8, 20, 23, and 24). They appear electron-opaque, but because of the over-all opacity of the peroxisome, as well as uncertainty concerning the validity of the method at the molecular level (see footnote 7), it is premature to suggest that catalase is represented by or concentrated in these substructures. The inner structures of the peroxisomes bear some resemblance to the more evident fibrils and threads recently described in the peroxisomes of some grasses studied by Frederick and Newcomb (21).

Fine threads or strands may also be seen at the periphery of the peroxisomes, just inside the delimiting membranes (Figs. 6–8). These sometimes appear as if extending to the adjacent smooth ER (Figs. 6 and 33).

ER, LYSOSOMES, AND PEROXISOMES: Without focusing our attention upon the matter, we have three times observed relatively small regions of ER to which small lysosomes (residual bodies) as well as peroxisomes are connected (Figs. 31 and 32).

Except for the cells at the tips of the villi, autophagic vacuoles are rarely encountered in the absorptive cells. In only a single instance was a peroxisome seen within an autophagic vacuole.

FIGURE 16 Guinea pig duodenum. Fixed in glutaraldehyde-formaldehyde. There are a few ribosomes, both ER-bound (lower *R*) and free (upper *R*), near the periphery of the peroxisome cluster. Within the cluster virtually all ER membranes are smooth. Continuities between peroxisomes and SER are indicated by arrowheads. × 41,000.

FIGURE 17 Guinea pig duodenum. Fixed in glutaraldehyde-formaldehyde. Incubated in DAB medium, pH 9.0, for 100 min. The arrows indicate a dilated region of tortuous SER within which the characteristic tubular structures of peroxisomes are discernible. There is relatively little density in the peroxisome. Possibly full condensation of material has not yet occurred. Another possibility is that the condensed material is sectioned superficially. × 102,000.

FIGURE 18 Guinea pig jejunum. Fixed in OsO_4–phosphate. The entire length of SER, turning upward from the lower to the upper arrow, appears as a tortuous structure with dilatations. The dilatations may form more distinct peroxisomes such as No. 1 and No. 2. Arrowheads indicate continuities of peroxisomes with SER. Within the dilated areas structures characteristic of peroxisomes are visible; cf. Fig. 17. × 34,000.

FIGURE 19 Guinea pig duodenum. Fixed in OsO_4–glutaraldehyde. This area is unusually rich in ribosomes (*R*), both ER-bound and free. Arrowheads mark membrane continuities between peroxisomes No. 1 and No. 3 and SER; note that in both instances the SER joins RER, marked by ribosomes. The arrow is directed towards internal circular structures. × 50,000.

FIGURE 20 Guinea pig ileum. Fixed in glutaraldehyde. Incubated in DAB medium, pH 9.0, for 100 min. Ribosomes or spicules (see text) are present at *R* but elsewhere the ER is smooth. Peroxisomes No. 1 and No. 2 show irregular material within them (arrows). At No. 2, the ER may be dilating to form a peroxisome. × 65,000.

FIGURE 21 Guinea pig duodenum. Fixed in glutaraldehyde. Incubated in DAB medium, pH 9.0, for 100 min. Ribosomes are seen at *R*. Arrowheads indicate membrane continuities between peroxisomes and SER. × 74,000.

FIGURES 22–24 Guinea pig ileum. Fixed in glutaraldehyde. Incubated in DAB medium, pH 9.7, for 100 min. Except for a few ribosomes or spicules (see text) seen at *R*, all of the ER is smooth. Irregular structures are seen within all peroxisomes; arrows indicate some that are more evident. A few strands between SER and a peroxisome are seen in Fig. 23 at the bottom left of peroxisome No. 1. The tripartite nature of the delimiting membranes of the peroxisomes is seen in Fig. 23. Because of their tortuosities the membranes show apparent "breaks" and larger areas where the membranes appear to be lacking. Arrowheads indicate where continuities of peroxisomes and SER are visible. Fig. 22, × 64,000; Fig. 23, × 74,000; Fig. 24, × 77,000.

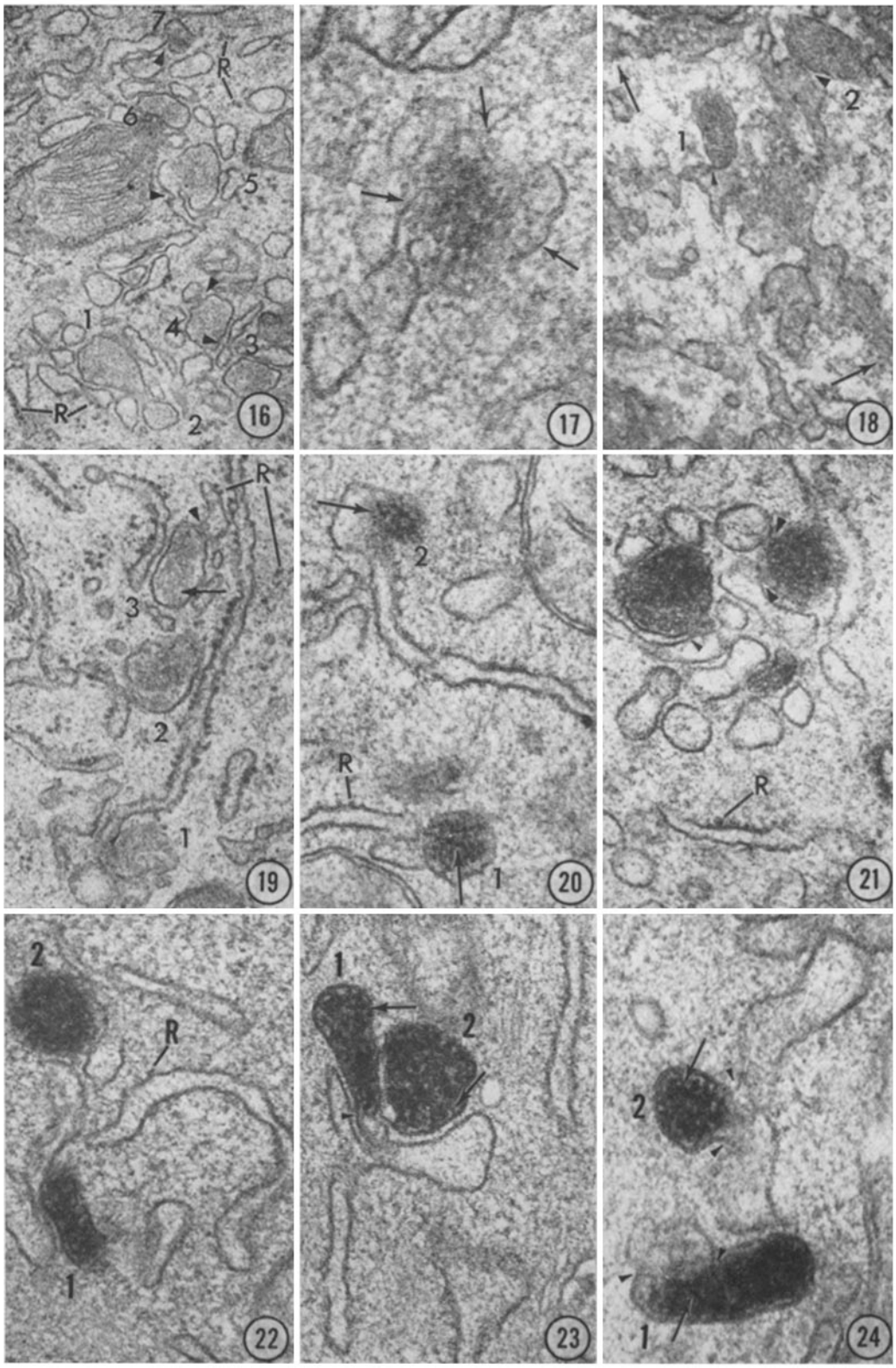
7
R
6
5
1
4
3
R
2
16
17
2
1
18
R
3
2
1
19
2
R
1
20
R
21
2
R
1
22
1
2
23
2
1
24

OTHER FEATURES SEEN TO ADVANTAGE BY TILTING SECTIONS: Several other observations, made incidentally and emphasizing the value of tilting thin sections in the electron microscope, are worth recording: (*a*) Delimiting membranes of lysosomes may be invisible at one tilt and become evident at another tilt (Figs. 31 and 32); (*b*) coated vesicles, often so small that they are present in only one of a series of consecutive serial sections (Figs. 25 and 26), may readily show their "vesicle in a basket" (36) character; (*c*) other membranes, such as those of ER (Figs. 31–33), autophagic vacuoles (Figs. 31 and 32), Golgi elements (Fig. 33), and mitochondria (Figs. 31 and 32), may more readily be observed; and (*d*) aspects of nuclear pores (Fig. 33) and lipoprotein particles may become more evident

Rat Duodenum

Our attention was focused exclusively on the peroxisomes and ER. Nevertheless it is apparent that rat duodenal cells show lipid droplets within the ER (Figs. 35 and 36) while such droplets are rarely seen in the guinea pig duodenal cells. On the other hand, in the guinea pig duodenal cells spherical bodies containing electron-opaque grains are larger and more numerous than in the rat.

The peroxisomes of rat duodenum have the same general distribution within the absorptive cells as in the guinea pig small intestine. None was seen near the terminal web; most are in the supranuclear cytoplasm. They often appear in clusters (Figs. 35 and 36). As in the guinea pig, the peroxisomes may reasonably be considered as locally dilated ER (Figs. 35 and 36; especially peroxisome No. 1 in Fig. 36). Ribosomes are always absent from the ER surface facing the peroxisomes. Only occasionally are a few ribosomes or spicule-like structures present in the regions of peroxisome clusters (Fig. 35). The inner structures of the peroxisomes resemble those in the guinea pig (cf. Figs. 35 and 36 with Figs. 21, 23, and 30).

We did not visualize the peroxisomes of the rat duodenum in the light microscope. The size of the peroxisomes is similar to that in the guinea pig, with about 75% ranging in diameter from 0.15 μ to 0.25 μ. It is not possible to quantitate the degree of DAB oxidation in electron micrographs, but our impression is that the rat duodenum peroxisomes are less DAB reactive than those of the guinea pig. We did not investigate whether the optimal conditions for the DAB reaction were the same for the rat as for the guinea pig.

DISCUSSION

Definition of Peroxisome and Microperoxisome; the Origin of Peroxisomes

It is remarkable that the historical advance in knowledge of the two cytoplasmic particles identified by Christian de Duve and collaborators

FIGURES 25–26 Guinea pig ileum. Fixed in OsO_4–phosphate. Two consecutive sections. A continuity between peroxisome No. 3 and SER is indicated by an arrowhead. Because of their small size, some peroxisomes are seen in only one of the two sections. Thus No. 6 and No. 7 are seen in Fig. 26 but not in Fig. 25. Similarly, it is not clear whether the peroxisomes indicated by the upper X in Fig. 26 corresponds to one or both of No. 4 and No. 5 in Fig. 25, and the lower X in Fig. 26 is one or both of No. 2 and No. 3 in Fig. 25. The same is true of coated vesicles: two are seen in Fig. 25 (arrows) but not in Fig. 26. Two small lysosomes are seen at *L*. In Fig. 25 a cluster of small vesicles is seen at *V*; one vesicle appears as if budding from SER. × 23,000.

FIGURES 27–28 Guinea pig jejunum. Fixed in OsO_4. Two of seven micrographs, taken of the same section at different angles, are shown; Fig. 27 at 0° and Fig. 28 at −30°. Continuities of peroxisomes and SER are seen in all seven micrographs; arrowheads mark continuities visible in the figures. The structure marked No. 5 is probably a cradle-like peroxisome, continuous with SER at both ends, viewed from above; the lower limb of SER shows its cisterna in the +20° micrograph (not illustrated). The internal structures of the peroxisomes are barely evident at this low magnification; compare with insets, Fig. 33. The irregular linear and circular aspects of the inner structures are indicated by arrows. The endoplasmic reticulum (*ER*) in this area is devoid of ribosomes except possibly at *R* which may be ribosomes or spicules (see text). × 36,000.

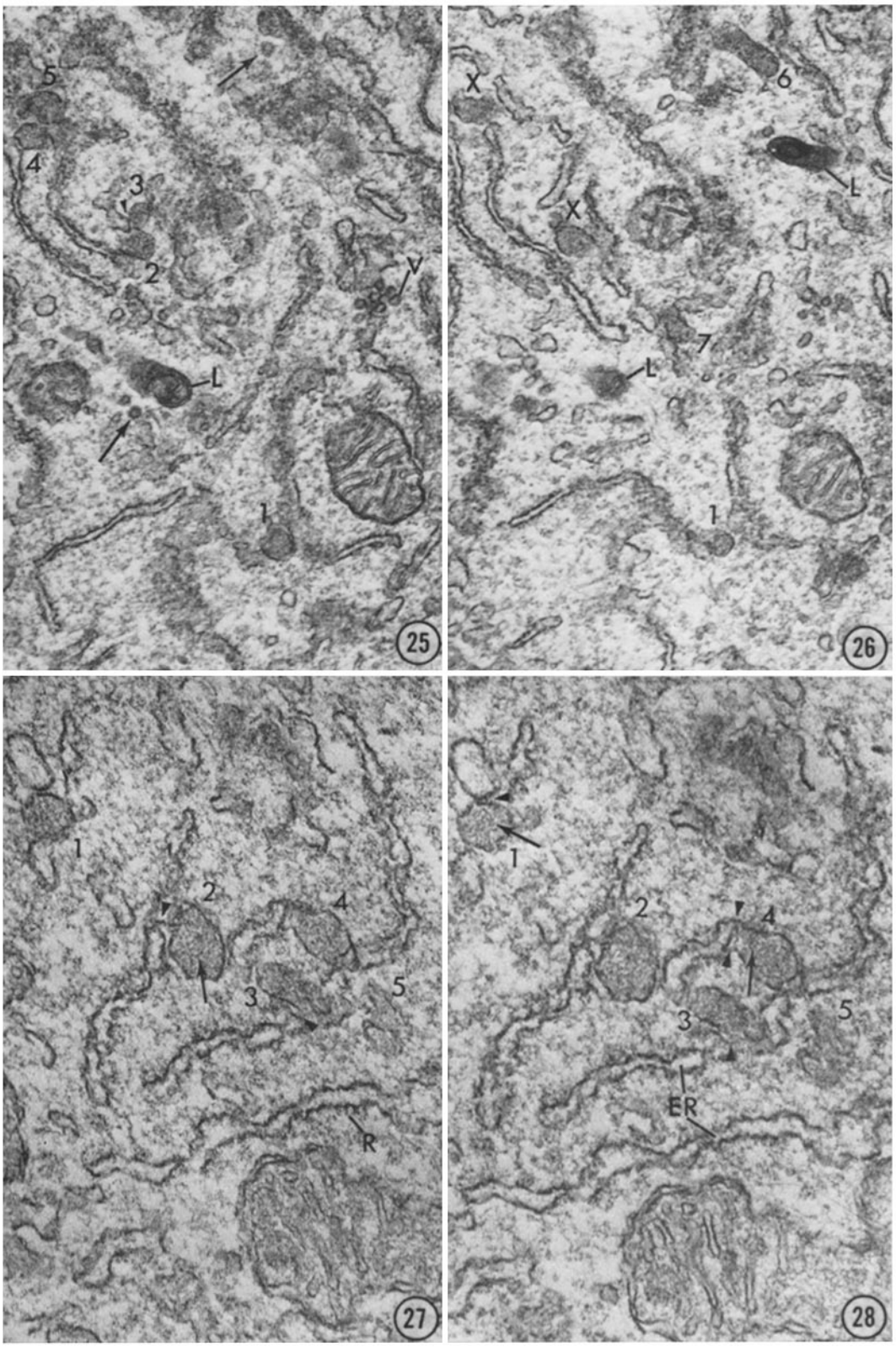
5
4
3
2
V
L
1
25
X
6
X
L
L
7
1
26
1
2
4
3
5
R
27
1
2
4
3
5
ER
28

show striking parallels. Originally a biochemical concept (13, 10), *lysosomes* were soon identified in the electron microscope in collaborative work by Novikoff, Beaufay, and de Duve (57). de Duve's biochemical definition of a lysosome was, and remains, a cytoplasmic particle which contains a collection of "latent" acid hydrolases. As biochemical work progressed, the number of hydrolytic enzymes sedimenting together from liver homogenates and characterized by acid pH optima increased from five to over 35. Of these only one, acid phosphatase, was readily available for reliable localization by cytochemistry. As early as 1960 one of us (51, 52) proposed a tentative cytological definition: the presence of an outer delimiting membrane and the demonstrability of acid phosphatase activity. Although the importance of showing other hydrolase activity within the same particle was recognized, this was possible only by light microscopy, and that only in the case of large lysosomes. For example, in the proximal convolution cells of mammalian kidney, thyroid epithelium and phagocytes pararosaniline procedures for other acid hydrolases could show their presence, as well as acid phosphatase, in the same particle (53, 54, 58). Two hydrolases other than acid phosphatase could be demonstrated at the electron microscope level, arylsulfatase and E 600-resistant esterase. However, because of several difficulties, their use has been limited. Thus, the acid phosphatase method remains the essential tool of cytologists in confirming the lysosomal nature of structures with characteristic appearances in the electron microscope. In discussing this history, in 1969 de Duve (10) wrote, "I must confess that Novikoff . . . received little encouragement on my part. I objected strongly to what I considered a misappropriation of the word *lysosome*, which in my own copyrighted version implied the presence of several acid hydrolases, and which he was now using to designate any structure giving a positive reaction for a single enzyme. Right was of course on my side, but pragmatism has won, since it is clear that we would still be groping our way into lysosomal physiology without the help of the cytochemical staining reaction for acid phosphatase."

Because of their large size and characteristic ultrastructure, *peroxisomes* were readily identified by electron microscopy in rat liver and kidney. This was particularly true in liver which possessed a large nucleoid or core. The peroxisomes were described as "microbodies." It was, however, relatively difficult to show the continuities of these peroxisomes with ER. There are still some (40, 84, 72, 18) who do not agree that such continuities exist in adult rat liver. Although an internal core is not always present (32) it is still often stated that peroxisomes show an "identifying core structure" (74). The initial biochemical characterization of peroxisomes rested on the presence in rat liver peroxisomes of catalase, which destroys H_2O_2, and two oxidases which produce H_2O_2, urate oxidase, and D-amino acid oxidase (12). When biochemical work was extended to other tissues and other organisms,

FIGURES 29–30 Guinea pig duodenum. Fixed in glutaraldehyde. Incubated in DAB medium, pH 9.7, for 90 min. Two consecutive sections. Peroxisomes No. 2 and No. 5 are present in Fig. 29 but little, if any, is seen of them in Fig. 30. A bit of No. 7 is seen in Fig. 29 but none is evident in Fig. 30. Peroxisome No. 9 is seen in Fig. 30 but not in Fig. 29. Arrowheads indicate continuities of peroxisomes and SER. Note that the mitochondria (*M*) are in their "condensed" form. A few ribosomes are seen at *R*. × 38,000.

FIGURES 31–32 Guiniea pig duodenum. Fixed in glutaraldehyde. Incubated in DAB medium, pH 9.7, for 90 min. Two of seven micrographs taken of the same section at different tilts, Fig. 31 at −30° and Fig. 32 at +30°. Arrowheads show continuities of SER and peroxisomes. Note the dependence upon the degree of tilt of the visibility of the lysosome (*L*) membrane and the appearance of the ER, e.g., near peroxisome No. 1. The short arrows in Fig. 32 indicate small breaks in the membrane of the lysosome (dense body) close to where it joins the SER membrane. These breaks are not present in the 0° micrograph; see Fig. 7, A. B. Novikoff and P. M. Novikoff, 4th International Congress of Histochemistry and Cytochemistry, Kyoto, Japan, 1972. See also Fig. 6 which shows continuity of peroxisome No. 2 with SER. A large lysosome, probably an autophagic vacuole, shows small portions of its delimiting membrane in both Figs. 31 and 32 (arrows); other portions were seen at tilts of −20°, −10°, and +20° (not illustrated). Other arrows in Fig. 31 indicate DAB reaction product in the mitochondrial cristae; in Fig. 32 the cristae are blurred. Ribosomes or spicules (see text) are seen at *R*. × 36,000.

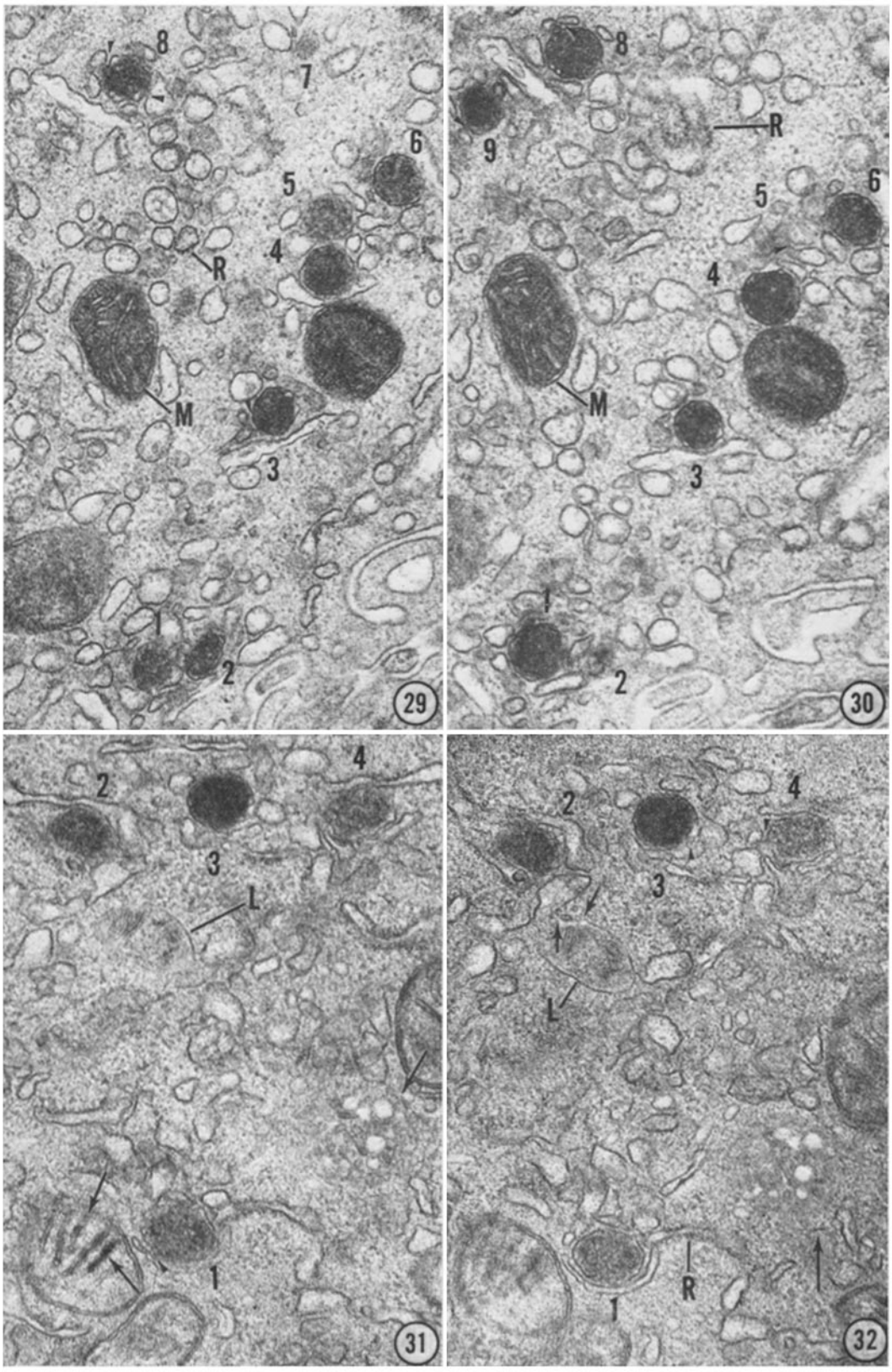
8
7
6
5
4
R
M
3
1
2
29
8
9
R
6
5
4
M
3
1
2
30
2
4
3
L
1
31
2
4
3
L
R
1
32

marked variability in the content of H_2O_2–producing oxidases was observed. Thus, the biochemical definition of peroxisome was modified: a cytoplasmic particle (with specified sedimentation characteristics) which "possess at least one hydrogen peroxide–producing oxidase together with catalase" (11). A recent publication on *Euglena gracilis* raises the possibility that the definition may require further modification. Graves et al., (28) find peroxisome-like particles in electron micrographs of these cells, particularly when grown on 2-carbon sugars. The authors suggest, but do not demonstrate, that glyoxylate pathway enzymes, used by *Euglena* in the metabolism of exogenously provided 2-carbon sugars, are localized within these particles. Yet the particles apparently lack catalase. They are unreactive after incubation in an alkaline DAB medium, essentially that of Novikoff and Goldfischer (59). The authors refer to unpublished results showing the absence of catalase activity, measured biochemically. Confirmation of the catalase results and the suggested localization of H_2O_2–producing oxidases in these particles will be awaited with much interest.

It is fortunate that the remarkably reliable cytochemical reagent, DAB, introduced into cytology for another purpose by Graham and Karnovsky (27), can readily be used for demonstrating catalase, the common denominator of peroxisomes thus far, with the possible exception referred to above (59, 29, 17). Although not totally free of bleeding from high accumulations to adjacent structures[7], DAB oxidation product diffuses from sites of production far less than does lead phosphate during incubation for acid phosphatase activity. False negatives and false positives may occur readily in acid phosphatase preparations, but relatively rarely in DAB cytochemistry.

As with lysosomes, peroxisome cytochemistry is, unfortunately, dependent largely upon one procedure, in this case, the alkaline DAB procedure. Neither the 3-amino-9-ethyl-carbozole procedure of Graham and Karnovsky (26) for urate oxidase nor the tetrazolium procedure of Allen and Beard (1) for α-hydroxy acid oxidase [even when the latter is improved as by Shnitka and Talibi (76) or by us] is presently useful for electron microscopy. The situation may change soon, since Shnitka and Talibi (76) have succeeded in showing α-hydroxy butyrate oxidase at the electron microscope level, in the large rat kidney peroxisomes. At the moment, then, only these kidney peroxisomes meet de Duve's

[7] We have often noted what we interpret as the bleeding of oxidized DAB from erythrocytes into small vesicles of adjacent capillary endothelial cells, and from eosinophil granules into adjacent cytoplasm. We consider such bleeding to be the major cause of ribosomal staining reported by some investigators (40, 84, 72, 18, 79). It would appear that bleeding is responsible for the filling with reaction product of the areas within the cristae and between the inner and outer membranes of mitochondria (75). See also Beard, M. E., and A. B. Novikoff, A comparison of two diaminobenzidine procedures for visualizing mitochondria, in preparation.

FIGURE 33 Guinea pig jejunum. Fixed in OsO_4. In this series, fourteen micrographs were taken of the same section, tilting the stage at 0°, and after rotating the stage 83°. Of the fourteen, only three are illustrated: A, without rotation, tilted at −30°; B, without rotation, untilted; and C, rotated 83°, tilted at +30°. Six peroxisomes are seen. Continuities with SER are indicated by arrowheads. Internal peroxisomal structures are barely evident at this low magnification. They show better in the insets which include enlargements of No. 3 and No. 4. The irregular linear aspects of the internal structures are best suggested within No. 1 in A and B, within No. 2 in C, within No. 3 in A (inset) and B (inset), within No. 4 in A (inset), and within No. 5 in A and C. The circular aspects of the internal structures are best suggested within No. 1 in B and C, No. 3 in A and C (insets), No. 4 in C (inset), No. 5 in A and C, and No. 6 in C. The ER is devoid of ribosomes. The tripartite nature of the ER membrane is clearly seen in areas, and in the insets. Note: (*a*) the different appearances in the three micrographs of the regions of ER surrounding peroxisomes No. 1–No. 3 and No. 5 and in other areas of ER such as at the arrow; (*b*) that only in C can the parallel nature of the membranes delimiting the Golgi elements (*G*) be seen; and (*c*) the different appearances in the three micrographs of the nuclear pore (*P*) (the tripartite nature of the adjacent nuclear membrane is best seen in an unillustrated micrograph, −20° tilt at 83° rotation), and microfilaments (*M*). × 39,000; insets × 78,000.

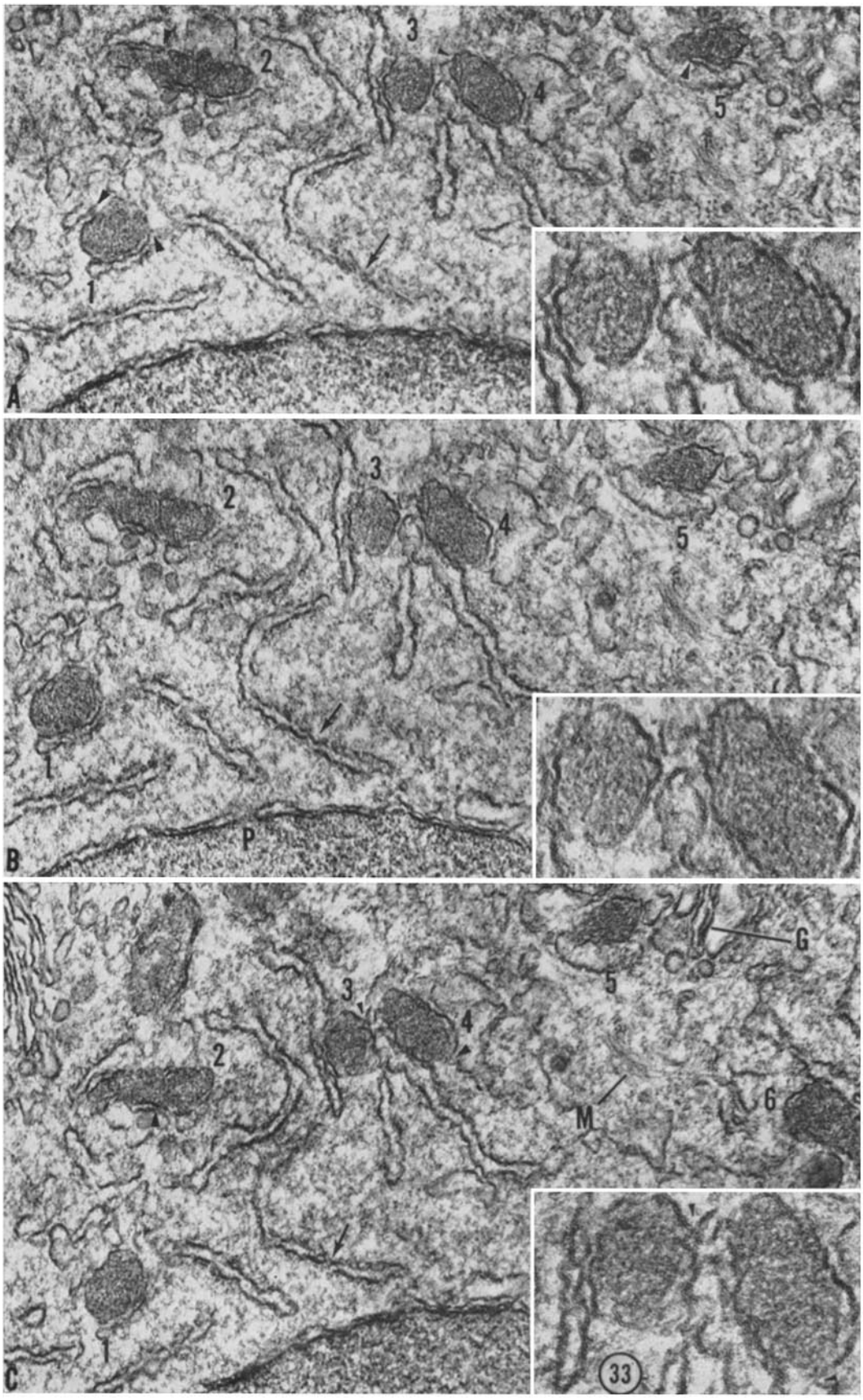
1
2
3
4
5
A
1
2
3
4
5
P
B
1
2
3
4
5
G
6
M
C
33

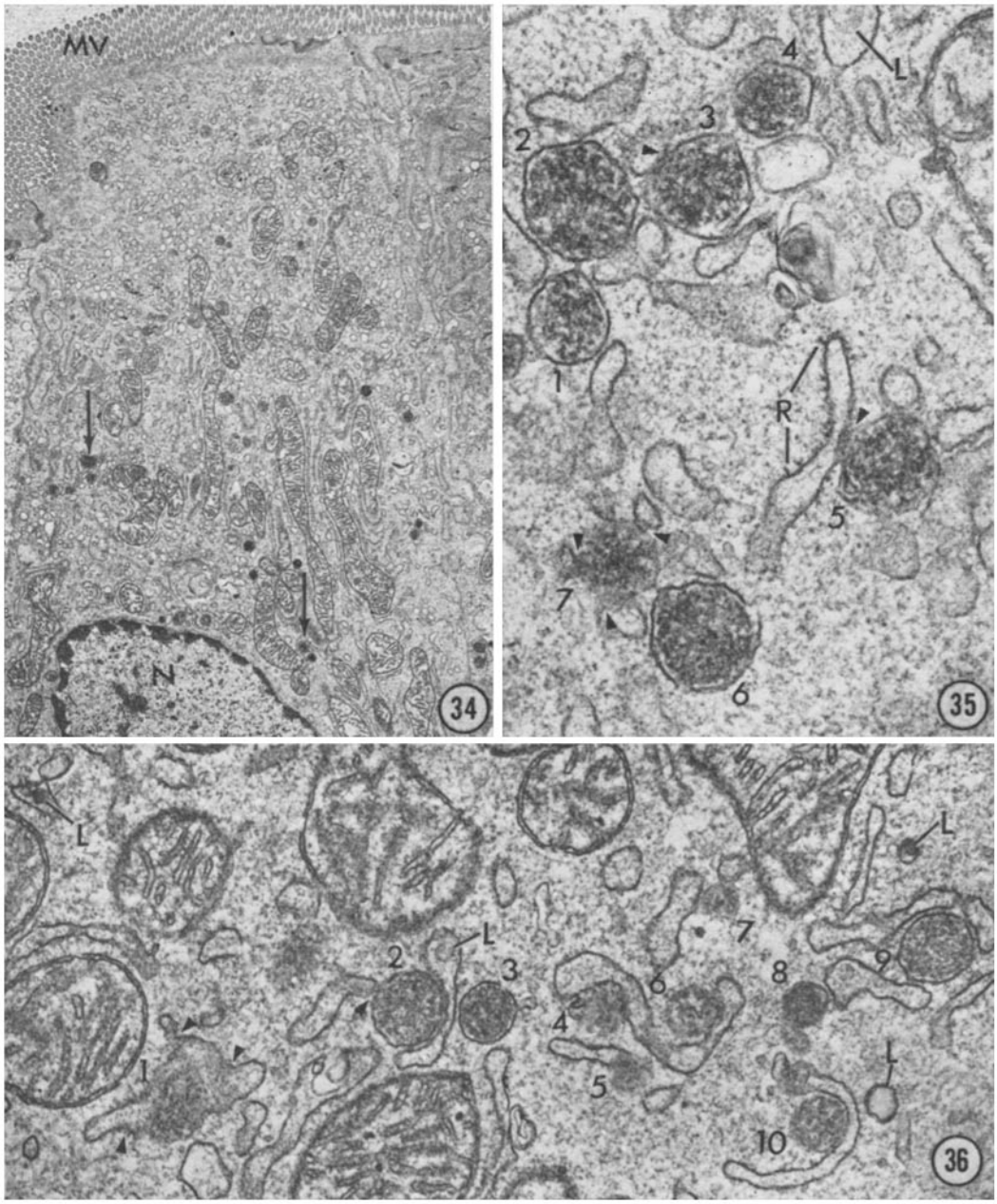

FIGURES 34–36 Rat duodenum. Fixed in glutaraldehyde. Incubated in DAB medium, pH 9.7, for 120 min.

FIGURE 34 Low power micrograph of supranuclear area. A portion of the nucleus is seen at *N* and microvilli at *MV*. The arrows indicate two of the numerous peroxisomes; note the ER adjacent to them. × 4200.

FIGURE 35 A portion of ER shows ribosomes or spicules (see text) (*R*) on the surface facing away from peroxisome No. 5. On the other surface, most of the ER is devoid of ribosomes. Arrowheads indicate continuities of peroxisomes and SER. The tripartite nature of the delimiting membranes is seen in areas of peroxisomes No. 2–No. 4 and No. 6. Wavy structures and linear and circular profiles are visible within the peroxisomes. A lipid droplet inside the ER is indicated by *L*. × 45,000.

FIGURE 36 Ten peroxisomes are seen in this cluster. Arrowheads indicate continuities of the delimiting membranes of peroxisomes with SER. Peroxisome No. 1 appears as a dilated region of ER. Note the irregular structures within No. 1 and other peroxisomes. Lipid droplets within the ER are indicated by *L*; note the proximity of one such droplet to peroxisome No. 2. × 33,000.

strict biochemical criteria through cytochemistry. Yet the cytochemical and cytological criteria for peroxisomes are firm enough for study of their roles in cell physiology and cell pathology. In the case of guinea pig and rat small intestine there are biochemical data, from Connock and Pover (8) and from Peters (62, 63), demonstrating particulate catalase (see Addendum).

In addition to the cytochemical test for catalase, fine structure is an extremely important basis for identifying peroxisomes. Our thesis is that the well-known peroxisomes of liver and kidney, those seen by early electron microscopists and probably constituting major portions of purified cell fractions separated from rat liver and kidney homogenates, differ in fine structure from peroxisomes in most other cell types. The peroxisomes of cells other than those of kidney (cells of proximal convolutions) and liver (hepatocytes) (and also the peroxisomes of the larval fat body of the insect, *Calpodes ethlius* [42]) are remarkably similar ultrastructurally, considerably more so than are the lysosomes of different cell types. Like the peroxisomes of the intestinal cells, they are small, they show no nucleoid or core, and they have intimate relations with the ER, including multiple continuities when carefully examined. Among these cells described by other investigators are those of *Tetrahymena pyriformis* (83, 48), perianal glands of the dog (37), cells of the distal convoluted tubules and collecting tubules of rat kidney (7), mouse and rat lung cells (64), rat adrenal cortex (5), and *Euglena* (28). Work from our laboratory, being prepared for publication, extends the list of cell types to include guinea pig esophagus, stomach (parietal and zymogenic cells), caecum, colon, rectum, eosinophils, fibroblasts, capillary endothelium, and various portions of the kidney tubules. In all, the peroxisomes are strikingly similar. Furthermore, in all but *Tetrahymena* and *Euglena* and perianal glands, the presence of catalase has been demonstrated by a positive incubation reaction in alkaline DAB media and by inhibition of the DAB reaction by AT. Finally, unlike the larger peroxisomes which apparently retain only limited connections with the ER, as an "appendage" (66), these peroxisomes may indeed be considered as local swollen areas of ER in which high concentrations of peroxisomal constituents are maintained.

We consider that these characteristics establish the peroxisomes of these cells (one may confidently predict their discovery in other cell types) as different enough from the original peroxisomes of liver and kidney to warrant a new name. Because we find it more difficult to give them a simple name which would stress the ER relationship we have chosen the term, microperoxisome. This name emphasizes their small size and their role as progenitor of the larger peroxisomes of liver and kidney.

Reddy and Svoboda (69) have reported important observations on the livers of genetically acatalasemic mice treated with ethyl chlorophenoxyisobutyrate (CPIB). CPIB treatment induces a rapid increase in peroxisome numbers. We would interpret these as microperoxisomes, judging from the multiple continuities of the peroxisomes with the ER and their small size. They also resemble the intestinal microperoxisomes in their arrangement in clusters in areas of local "degranulation and disaggregation" (69) of the ribosomes from the ER which dilates to form the microperoxisome.

Reddy and Svoboda (69) exercise caution in extending to normal animals their observations on mice with a genetic abnormality in catalase, a peroxisomal enzyme, after treatment with a drug, CPIB, affecting the ER. However, unpublished observations in our laboratory show large numbers of similar microperoxisomes in the livers of untreated normal adult rats. In addition, preliminary observations on the proximal convoluted cells in kidneys of such rats suggest that there, too, the large peroxisomes develop by enlargement of microperoxisomes.

After this manuscript was written we became aware of a 1968 publication on plant "microbodies" by Frederick et al. (22). The thesis developed by these authors is like the one we have outlined. They describe the presence in root meristem cells of numerous organelles remarkably like those for which we suggest the term microperoxisome [see also Fig. 3 in Poux (68)]. The organelles are small. They have an intimate relation with the ER which is present alongside of the microbody and lacks ribosomes on the surface adjacent to the organelle. They lack cores and their matrix is described as granular or fibrillar. Such plant microperoxisomes are also found in differentiated parenchyma cells which have the larger, better-known peroxisomes with cores ("typical microbody appearance" [22]). The larger core-containing microbodies are considered to "arise as differentiations of microbodies of the non-crystalline type" and to possess a less intimate relation to the ER. The plant core-containing peroxisomes are con-

sidered "a specialized type of microbody" in the same sense that we consider the large hepatic and renal peroxisomes as specialized.

Our observations on intestinal cells are consistent with the conclusion of Lazarow and de Duve (38, 39) that in rat liver the production of authentic, i.e., enzymatically active, catalase occurs in the peroxisome itself and not on ribosomes. Presumably, precursors of the final catalase molecules are transported from the ribosomes via the ER to the microperoxisomes. In the intestinal absorptive cells ribosomes are conspicuously absent from the membranes of the microperoxisomes and adjacent ER. No support is found for the view that ribosomes carry enzyme directly to the peroxisomes without ER involvement. We consider it likely that the reported staining of ribosomes adjacent to peroxisomes is due to diffusion of oxidized DAB generated within the peroxisome (see footnote 7). The adsorption of the diffusing reaction product is nonspecific: the ER membrane to which the ribosomes are attached is also stained.

Isolated Organelles and Turnover Data

In 1964 Novikoff and Shin (60) speculated about the origin of microbodies (peroxisomes) in rat hepatocytes and raised the possibility that "material of increased electron density becomes localized in areas of the endoplasmic reticulum. As the material accumulates the regions bulge into one or several elliptical areas (microbodies appear in clusters) which swell and separate from the endoplasmic reticulum . . . or . . . the extensions may actually be continuing connections between endoplasmic reticulum and microbodies. Such connections may be broken during homogenization thus enabling isolation of the microbodies by centrifugation".

Strong evidence for the origin of peroxisomes from the ER in hepatocytes (of acatalasemic mice treated with CPIB) was published by Reddy and Svoboda (69). They believe that homogenization separates peroxisomes from the ER. They also raise an interesting possibility that would complicate biochemical assays: "On homogenization, the membranes rupture and appear to enclose varying quantities of microbody protein material (this can account for the differences in size of the isolated particles), thereby facilitating their isolation as distinct particles." Whether loss of peroxisomal protein does indeed occur during homogenization remains to be demonstrated.

Another possibility may now be raised, namely that in hepatocytes the microperoxisomes and the core-containing peroxisomes may respond differently during the homogenization and isolation procedures. Because of their large numbers and cytological uniformity, biochemical study of intestinal microperoxisomes should prove important.

The concept that dilated portions of ER contain localized high concentrations of catalase and other peroxisomal proteins is consistent with the turnover data of Poole and coworkers (65–67). These data establish the half-life for catalase and other peroxisomal proteins in rat hepatocytes to be 1.6–2.2 days. Since the pool of peroxisomal proteins is readily accessible to all peroxisomes, independent of size of isolated particles, the possibility that "the peroxisomes within a liver cell exist as individuals" (66) is made highly unlikely. Alternative possibilities of explaining the turnover data in Poole et al. (66) could include the complex relation of microperoxisomes to ER. Attention needs now to be focused on two classes of peroxisomes in hepatocytes, the microperoxisomes and the larger core-containing peroxisomes.

Microperoxisomes in Absorptive Cells of the Small Intestine

It is impressive that organelles so numerous in intestinal epithelial cells as the microperoxisomes should have escaped the attention of electron microscopists. As far as we are aware, peroxisomes of these cells have not been previously described. In 1966 Yamamoto (85) published electron micrographs of goldfish and trout intestinal epithelia which include what appear to be microperoxisomes. The author considered them as "small membrane-bounded bodies containing a light staining granular substance which bear some resemblance to secretory granules". In their extensive 1968 report of mouse, rat, hamster, and guinea pig intestinal epithelia, Hugon and Borgers (34) mention microbodies, i.e., peroxisomes: "In the hamster, dense granules with an organized core, interpreted as microbodies were sometimes noted". Probably the small size and the absence of cores account for the failure of electron microscopists to note the presence and abundance of microperoxisomes. Three recent studies involving incubation in DAB media for peroxidase activity (not catalase) do not refer to peroxisomes: in guinea pig small intestine ("random" samples) (71), rat jejunum and ileum (9), and mouse duodenum (33).

The work reported here, like all morphological and cytochemical studies on peroxisomes, rests on biochemical studies which have established the presence of catalase in peroxisomes of diverse cell types (see reference [31] for summaries of work from the laboratories of de Duve and others). Recent studies of "peroxisome-like bodies", microperoxisomes by the criteria described above, have utilized the oxidation of DAB at alkaline pH to reveal the presence of catalase. For light microscope observations of these small organelles, in small intestine and other tissues, we have had to modify the optimal media for staining peroxisomes (59) in order to yield stronger specific staining while removing all the mitochondrial staining which tends to mask the microperoxisomes. The new procedure, and results obtained with it in other cell types, are described elsewhere[1].

We have only studied the absorptive cells of guinea pig small intestine and of rat duodenum. However, it is highly unlikely that these two species are unique among mammals with respect to the presence of microperoxisomes in these cells. Indeed, in a recent paper by Hugon et al. (35) on glucose-6-phosphatase localization in mouse intestine, Fig. 6 shows a cluster of about ten microperoxisomes, unidentified in the legend.

The absorption of lipid from the intestinal lumen and its transport, with modification to form chylomicra, is a major function of the absorptive cells of the small intestine (6). Peroxisomes have been implicated in lipid metabolism (25). We are currently studying the effect on microperoxisomes of feeding lipids to fasted guinea pigs and rats. Will an increased demand on lipid-metabolizing enzymes lead to changes in microperoxisomes, in addition to changes reported in the endoplasmic reticulum and Golgi apparatus?

In considering possible physiological roles of D-amino acid oxidase of peroxisomes, de Duve (11) has called attention to the report that the oxidase is absent in the kidney of germ-free mice and is induced when dead bacteria are fed to the rats (45). He reasons that the D-amino acid of the bacteria must pass through the circulation, from intestine to kidney. It would be of interest to see whether isolated intestinal microperoxisomes have D-amino acid oxidase activity (see Addendum). We plan to study these organelles in germ-free guinea pigs and rats, to compare them with those we have found in the normal animals, and also to see the effect of feeding dead bacteria to the germ-free animals.

Other Features of ER Function

If, indeed, peroxisomes are dilated regions of the ER, what kinds of controls operate to channel peroxisomal enzymes into the peroxisomes and to retain them there while excluding, e.g., lysosomal enzymes? As Figs. 31 and 32 indicate, a peroxisome and a lysosome may be attached to virtually the same ER region. In addition, particularly in the rat duodenum, there may be lipid droplets moving through neighboring, perhaps the same, portions of ER (Fig. 36). In the guinea pig duodenum, where we have observed GERL, an acid phosphatase-rich portion of ER at the inner aspect of the Golgi apparatus (61), large amounts of acid phosphatase and presumably other lysosomal hydrolases are transported to this region of ER. The extent to which ER channeling appears necessary staggers our present imagination.

In our laboratory, as in others, evidence from DAB cytochemistry has been sought for the transport of catalase through the ER. Thus far, the ER has proved to be negative, even under conditions where the number of peroxisomes is increasing rapidly. This might readily be explained by Lazarow and de Duve's finding (38, 39) that in rat liver enzymatically active catalase is produced from precursor molecules within the peroxisome itself. If an apocatalase does not acquire its heme component until it reaches the peroxisome, then staining with an optimal DAB medium for catalase would occur in the peroxisome but not in the ER. On the other hand, were a hemoprotein precursor of catalase transported by the ER, this could, in principle, be detectable by incubation in a proper DAB medium, with special pH, H_2O_2, or other requirements (55, 56). An ER hemoprotein would still be undetectable by cytochemistry if its concentration were too low. Publication of detailed cell fractionation studies, in progress (39), may clarify the problem.

Peroxidase Activity in Small Intestine

As already noted, our finding of large numbers of microperoxisomes with DAB reactivity, usually inhibitable by AT, at alkaline pH, in both guinea pig and rat small intestine is consistent with the biochemical findings by Connock and Pover (8) and Peters (62, 63; also see Addendum). It is well known, however, that DAB oxidation is nonspecific (55, 56). Indeed, peroxidase was the first hemoprotein to be visualized by DAB (27); see Fig. 2. In addition, there are biochemical data which

show small intestine to be rich in peroxidase activity (50). Unfortunately, assessment of these data in terms of absorptive cells is difficult because the preparations undoubtedly contain many eosinophil granules which are rich in peroxidase (2). Stelmaszyńska and Zgliczyński (78) have recently purified a peroxidase from hog intestine. Its properties are those of eosinophil peroxidase. The authors ascribe the enzyme exclusively to the eosinophils of the connective tissue.

Three publications in 1971 report the absence of endogenous peroxidase activity, in cytochemical preparations, in the absorptive cells in the small intestine: in guinea pig (71), rats (9), and mice (33). However, these reports are not compelling. The tissues were used as controls in experiments designed to follow the fate of exogenously provided horseradish peroxidase. The sections were incubated at room temperature in a suboptimal DAB medium. Such incubation suffices for revealing the exogenous peroxidase but not the endogenous peroxidases thus far reported except for that in eosinophil granules. Although the pH 7.6 medium (81) which we employed for electron microscopy of rat ileum is somewhat less optimal than the medium usually employed in our laboratory (55, 56), it readily reveals the presence of peroxidase in the ER of the crypt cells in rat colon as well as the peroxidase of eosinophil granules. Yet the microperoxisomes of guinea pig ileum show no reaction product in this medium.

Additional observations strengthen the conclusion that a true peroxidase contributes very little, if anything, to the DAB reactivity of absorptive cell microperoxisomes after incubation of sections at alkaline pH. In addition to high pH, peroxidases of epithelial cells (rat colon and thyroid, parotid, and submaxillary glands) are inhibited by high levels of H_2O_2 or KCN. Microperoxisomes are more reactive at pH 9.7 than 9.0. They are unaffected by 0.3% H_2O_2 or 1×10^{-2} M KCN. Finally, 2,6 DCPIP, which has no effect upon DAB reactivity of peroxidase in the cells of rat colon epithelium, and very little, if any, upon the peroxidase of eosinophil granules, totally inhibits the reactivity of ileum microperoxisomes.

Biochemical assays of intestinal mucosal cells (or of villi separated from crypts so as to eliminate the eosinophils) would be highly desirable in order to establish more directly the absence of true peroxidase activity in microperoxisomes (see Addendum). The presence of some peroxidase as well as catalase in microperoxisomes would not, however, weaken their classification as peroxisomes[8]. In principle, it would parallel the situation of the azurophilic granules of rabbit neutrophils. When assayed biochemically, the granules display not only acid hydrolase activities but peroxidase activity as well (3). This does not exclude their classification as lysosomes.

It may be noted parenthetically that the eosinophils in guinea pig intestine possess microperoxisomes, with characteristic fine structure and with catalase activity as indicated by strong reactivity in alkaline DAB, as well as the much more numerous peroxidase-rich granules[1].

We are grateful to Cleveland Davis and Nelson Quintana for devoted and splendid assistance in these experiments. We wish also to thank Jack Godrich for preparation of the photographs, the Philips Electronic Instruments, Mount Vernon, N. Y., for making the Philips 300 microscope available to us, and Harry Walker and Irene Piscopo for assistance in using the goniometer stage. We acknowledge, with pleasure, the discussions with Dr. Christian de Duve, Dr. T. J. Peters, and Mr. Paul Lazarow of the Rockefeller University, of unpublished results on peroxisomal enzymes in the guinea pig intestine and of data on rat liver which bear on the possibility of detecting catalase in the ER cytochemically.

This work was supported by United States Public Health Service Research Grant R01-CA-06576. A. B. Novikoff is the recipient of United States Public Health Service Research Career Award K6-CA-14923 from the National Cancer Institute.

Received for publication 12 November 1971, and in revised form 18 January 1972.

ADDENDUM

Dr. T. J. Peters (private communication) has recently studied a particulate fraction obtained from homogenates of isolated epithelial cells of guinea pig jejunum. The fraction shows D-amino acid oxidase activity as well as catalase activity. The level of catalase activity of the particles is too high to permit valid measurements of peroxidase activity.

Since submission of this manuscript another cell type has been shown to possess cytoplasmic granules which give a positive reaction, inhibited by AT, when incubated in alkaline DAB. Ahlabo and Barnard (*J. Histochem. Cytochem.* 1971. **19**:670) describe these "peroxisomes" in brown fat cells as

[8] From differences in staining reactions Goldfischer and Essner (24) conclude that the hepatic and renal peroxisomes of acatalasemic mice possess true peroxidase rather than catalase.

ranging in size from 1.0 to 0.1 μ and lacking nucleoids. As in other descriptions of "peroxisome-like particles," their relation to the ER is unclear from the published micrographs.

Hruban et al. (*Lab. Invest.* 1972, **26**:86) describe "focal dilations" of ER in cells of Morris hepatomas that may well be microperoxisomes (Figs. 2, 3, 5, and particularly Fig. 13). Many of the peroxisomes illustrated to appear to be microperoxisome.

REFERENCES

1. ALLEN, J. M., and M. E. BEARD. 1965. α-Hydroxy acid oxidase: Localization in renal microbodies. *Science (Washington).* **149**:1507.
2. ARCHER, G. T., G. AIR, M. JACKAS, and D. B. MORELL. 1965. Studies on rat eosinophil peroxidase. *Biochim. Biophys. Acta.* **99**:96.
3. BAGGIOLINI, M., J. G. HIRSCH, and C. DE DUVE. 1970. Further biochemical and morphological studies of granule fractions from rabbit heterophil leukocytes. *J. Cell Biol.* **70**:586.
4. BAKER, J. R. 1946. The histochemical recognition of lipine. *Quart. J. Microsc. Sci.* **87**:441.
5. BEARD, M. E. 1971. Identification of peroxisomes in the rat adrenal cortex. *J. Histochem. Cytochem.* In press.
6. CARDELL, R. R., JR., S. BADENHAUSEN, and K. R. PORTER. 1967. Intestinal triglyceride absorption in the rat. An electron microscopical study. *J. Cell Biol.* **34**:123.
7. CHANG, C. H., B. SCHILLER, and S. GOLDFISCHER. 1971. Small cytoplasmic bodies in the loop of Henle and distal convoluted tubule that resemble peroxisomes. *J. Histochem. Cytochem.* **19**:56.
8. CONNOCK, M., and W. POVER. 1970. Catalase particles in the epithelial cells of the guinea-pig small intestine. *Histochem. J.* **2**:371.
9. CORNELL, R., W. A. WALKER, and K. J. ISSELBACHER. 1971. Small intestinal absorption of horseradish peroxidase. *Lab. Invest.* **25**:42.
10. DE DUVE, C. 1969. The lysosome in retrospect. *In* Lysosomes in Biology and Pathology. J. T. Dingle and H. B. Fell, editors. North Holland Publishing Co., Amsterdam. **I**:3.
11. DE DUVE, C. 1969. Evolution of the peroxisome. *Ann. N. Y. Acad. Sci.* **168**:369.
12. DE DUVE, C., and P. BAUDHUIN. 1966. Peroxisomes (microbodies and related particles). *Physiol. Rev.* **46**:323.
13. DE DUVE, C., B. C. PRESSMAN, R. GIANETTO, R. WATTIAUX, and F. APPELMANS. 1955. Tissue fractionation studies. VI. Intracellular distribution patterns of enzymes in rat liver tissue. *Biochem. J.* **60**:604.
14. ERICSSON, J. L. E., and B. F. TRUMP. 1966. Electron microscopic studies of the epithelium of the proximal tubule of the rat kidney. III. Microbodies, multivesicular bodies, and the Golgi apparatus. *Lab. Invest.* **15**:1610.
15. ESSNER, E. 1967. Endoplasmic reticulum and the origin of microbodies in fetal mouse liver. *Lab. Invest.* **17**:71.
16. ESSNER, E. 1970. Observations on hepatic and renal peroxisomes (microbodies) in the developing chick. *J. Histochem. Cytochem.* **18**:80.
17. FAHIMI, H. D. 1969. Cytochemical localization of peroxidatic activity of catalase in rat hepatic microbodies (peroxisomes). *J. Cell Biol.* **43**:275.
18. FAHIMI, H. D. 1971. Morphogenesis of peroxisomes in rat liver. Abstracts of the American Society of Cell Biology. New Orleans, La. 87.
19. FARQUHAR, M. G., and G. E. PALADE. 1965. Cell junctions in amphibian skin. *J. Cell Biol.* **26**:263.
20. FREDERICK, S. E., and E. H. NEWCOMB. 1969. Cytochemical localization of catalase in leaf microbodies (peroxisomes). *J. Cell Biol.* **43**:343.
21. FREDERICK, S. E., and E. H. NEWCOMB. 1971. Ultrastructure and distribution of microbodies in leaves of grasses with and without CO_2-photorespiration. *Planta.* **96**:152.
22. FREDERICK, S. E., E. H. NEWCOMB, E. L. VIGIL, and W. P. WERGIN. 1968. Fine-structural characterization of plant microbodies. *Planta.* **81**:229.
23. GOLDACRE, P. L., and A. W. GALSTON. 1953. The specific inhibition of catalase by substituted phenols. *Arch. Biochem. Biophys.* **43**: 169.
24. GOLDFISCHER, S., and E. ESSNER. 1970. Peroxidase activity in peroxisomes (microbodies) of acatalasemic mice. *J. Histochem. Cytochem.* **18**:483.
25. GOLDFISCHER, S., P. S. ROHEIM, and D. EDELSTEIN. 1971. Hypolipidemia in a mutant strain of "acatalasemic" mice. *Science (Washington).* **173**:65.
26. GRAHAM, R. C., JR., and M. J. KARNOVSKY. 1965. The histochemical demonstration of uricase activity. *J. Histochem. Cytochem.* **13**: 448.
27. GRAHAM, R. C., JR., and M. J. KARNOVSKY. 1966. The early stages of absorption of injected horseradish peroxidase in the proximal tubules of mouse kidney: Ultrastructural cytochemistry by a new technique. *J. Histochem. Cytochem.* **14**:291.
28. GRAVES, L. B., JR., L. HANZELY, and R. N. TRELEASE. 1971. The occurrence and fine structural characterization of microbodies in *Euglena gracilis. Protoplasma.* **72**:141.

29. HIRAI, K.-I. 1968. Specific affinity of oxidized amine dye (radical intermediater) for heme enzymes: Study in microscopy and spectrophotometry. *Acta Histochem. Cytochem.* **1**:43.
30. HIRSCH, J. G., and M. E. FEDORKO. 1968. Ultrastructure of human leukocytes after simultaneous fixation with glutaraldehyde and osmium tetroxide and "postfixation" in uranyl acetate. *J. Cell Biol.* **38**:615.
31. HOGG, J. F., editor. 1969. The nature and function of peroxisomes (microbodies, glyoxysomes). *Ann. N. Y. Acad. Sci.* **168**:209.
32. HRUBAN, Z., and M. RECHCIGL, JR. 1969. Microbodies and related particles. *Int. Rev. Cytol.* (Supplement I).
33. HUGON, J. S. 1971. Absorption of horseradish peroxidase by the mucosal cells of the duodenum of mouse. II. The newborn mouse. *Histochemie.* **26**:19.
34. HUGON, J. and M. BORGERS. 1968. Fine structural localization of acid and alkaline phosphatase activities in the absorbing cells of the duodenum of rodents. *Histochemie.* **12**:42.
35. HUGON, J. S., D. MAWSTRACCI, and D. MÉNARD. 1971. Glucose 6-phosphatase activity in the intestinal epithelium of the mouse. *J. Histochem. Cytochem.* **19**:515.
36. KANASEKI, T., and K. KODOTA. 1969. The "Vesicle in a Basket." A morphological study of the coated vesicle isolated from the nerve endings of the guinea pig brain, with special reference to the mechanism of membrane movements. *J. Cell Biol.* **42**:202.
37. KUHN, C. 1968. Particles resembling microbodies in normal and neoplastic perianal glands of dogs. *Z. Zellforsch. Mikrosk. Anat.* **90**:554.
38. LAZAROW, P. B. 1971. Biosynthesis of peroxisome catalase in rat liver. Abstracts of the American Society of Cell Biology. New Orleans, La. 161.
39. LAZAROW, P. B., and C. DE DUVE. 1971. Intermediates in the biosynthesis of peroxisomal catalase in rat liver. *Biochem. Biophys. Res. Commun.* **45**:1198.
40. LEGG, P. G., and R. L. WOOD. 1970. New observations on microbodies. A cytochemical study on CPIB-treated rat liver. *J. Cell Biol.* **45**:118.
41. LEIGHTON, F., B. POOLE, H. BEAUFAY, P. BAUDHUIN, J. W. COFFEY, S. FOWLER, and C. DE DUVE. 1968. The large-scale separation of peroxisomes, mitochondria, and lysosomes from the livers of rats injected with Triton WR-1339. Improved isolation procedures, automated analysis, biochemical and morphological properties of fractions. *J. Cell Biol.* **37**:482.
42. LOCKE, M., and J. T. MCMAHON. 1971. The origin and fate of microbodies in the fat body of an insect. *J. Cell Biol.* **48**:61.
43. LUCAS, F. V., H. A. NEUFELD, J. UTTERBACK, A. P. MARTIN, and E. STOTZ. 1955. The effect of estrogen on the production of a peroxidase in the rat uterus. *J. Biol. Chem.* **214**:775.
44. LUFT, J. H. 1961. Improvements in epoxy resin embedding methods. *J. Biophys. Biochem. Cytol.* **9**:409.
45. LYLE, L. R., and J. W. JUTILA. 1968. D-amino acid oxidase induction in germ-free mice. *J. Bacteriol.* **96**:606.
46. MILLER, F., and V. HERZOG. 1969. Die lokalisation von Peroxidase und sauer Phosphatase in eosinophilen Leukocyten während der Reifung. Elektronemikroskopisch - cytochem - ische Untersuchungen am Knochenmark von Ratte und Kaninchen. *Z. Zellforsch Mikrosk. Anat.* **97**:84.
47. MILLONIG, G. 1962. Further observations on a phosphate buffer for osmium solutions in fixation. *In* Proceedings of the 5th International Congress of Electron Microscopy. S. S. Breese, Jr., editor. Academic Press Inc., New York. **2**:8.
48. MÜLLER, M. 1969. Peroxisomes of protozoa. *Ann. N. Y. Acad. Sci.* **168**:292.
49. NEUFELD, H. A., F. V. LUCAS, A. P. MARTIN, and E. STOTZ. 1955. Peroxidase and cytochrome oxidase in the Walker Carcinoma 256. *Cancer Res.* **15**:550.
50. NEUFELD, H. A., A. N. LEVAY, F. V. LUCAS, A. P. MARTIN, and E. STOTZ. 1958. Peroidase and cytochrome oxidase in rat tissues. *J. Biol. Chem.* **233**:209.
51. NOVIKOFF, A. B. 1960. Biochemical and staining reactions of cytoplasmic constituents. *In* Developing Cell Systems and Their Control. D. Rudnick, editor. The Ronald Press Company, New York. 167.
52. NOVIKOFF, A. B. 1961. Lysosomes and related particles. *In* The Cell. J. Brachet and A. E. Mirsky, editors. Academic Press Inc., New York. **II**: 423.
53. NOVIKOFF, A. B. 1963. Lysosomes in the physiology and pathology of cells: Contributions of staining methods. *In* Ciba Foundation Symposium Lysosomes. A. V. S. de Reuck and M. P. Cameron, editors. Little, Brown and Company, Boston. 36.
54. NOVIKOFF, A. B. 1963. Lysosomes and possible roles in the reticuloendothelial system. *In* Role du Système Réticulo-endothélial dans l'Immunité Antibactérienne et Antitumorale. B. N. Halpern, editor. Centre National de la Recherche Scientifique, France. 67.

55. NOVIKOFF, A. B. 1970. Visualization of cell organelles by diaminobenzidine reactions. *7th Int. Congr. Electron Microsc.* Grenoble. **1**:565.

56. NOVIKOFF, A. B., M. E. BEARD, A. ALBALA, B. SHEID, N. QUINTANA, and L. BIEMPICA. 1971. Localization of endogenous peroxidases in animal tissues. *J. Microsc.* **12**:58.

57. NOVIKOFF, A. B., H. BEAUFAY, and C. DE DUVE. 1956. Electron microscopy of lysosome-rich fractions from rat liver. *J. Biophys. Biochem. Cytol.* **2**:179.

58. NOVIKOFF, A. B., E. ESSNER, and N. QUINTANA. 1964. Golgi apparatus and lysosomes. *Fed. Proc.* **23**:1010.

59. NOVIKOFF, A. B., and S. GOLDFISCHER. 1969. Visualization of peroxisomes (microbodies) and mitochondria with diaminobenzidine. *J. Histochem. Cytochem.* **17**:675.

60. NOVIKOFF, A. B., and W.-Y. SHIN. 1964. The endoplasmic reticulum in the Golgi zone and its relations to microbodies, Golgi apparatus and autophagic vacuoles in rat liver cells. *J. Microsc.* **3**:187.

61. NOVIKOFF, P. M., A. B. NOVIKOFF, N. QUINTANA, and J.-J. HAUW. 1971. Golgi apparatus, GERL, and lysosomes of neurons in rat dorsal root ganglia, studied by thick section and thin section cytochemistry. *J. Cell Biol.* **50**:859.

62. PETERS, T. J. 1970. The subcellular localization of di- and tri-peptide hydrolase activity in guinea-pig small intestine. *Biochem. J.* **120**: 195.

63. PETERS, T. J. 1972. Subcellular fractionation of the enterocyte with special reference to peptide hydrolases. *Ciba Foundation Symposium.* In press.

64. PETRIK, P. 1971. Fine structural identification of peroxisomes in mouse and rat bronchiolar and alveolar epithelium. *J. Histochem. Cytochem.* **19**:339.

65. POOLE, B. 1969. Biogenesis and turnover of rat liver peroxisomes. *Ann. N. Y. Acad. Sci.* **168**: 229.

66. POOLE, B., T. HIGASHI, and C. DE DUVE. 1970. The synthesis and turnover of rat liver peroxisomes. III. The size distribution of peroxisomes and the incorporation of new catalase. *J. Cell Biol.* **45**:408.

67. POOLE, B., F. LEIGHTON, and C. DE DUVE. 1969. The synthesis and turnover of rat liver peroxisomes. II. Turnover of peroxisome proteins. *J. Cell Biol.* **41**:536.

68. POUX, N. 1970. Reactions d'organites cellulaires avec la diaminobenzidine dans le méristème radiculaire de Cucumis sativus L. (Cucurbitacees). *7th Int. Congr. Electron Microsc.* Grenoble. **1**:571.

69. REDDY, J., and D. SVOBODA. 1971. Microbodies in experimentally altered cells. VIII. Continuities between microbodies and their possible biologic significance. *Lab. Invest.* **24**:74.

70. REYNOLDS, E. S. 1963. The use of lead citrate at high pH as an electron-opaque stain in electron microscopy. *J. Cell Biol.* **17**:208.

71. RHODES, R. S., and M. J. KARNOVSKY. 1971. Loss of macromolecular barrier function associated with surgical trauma to the intestine. *Lab. Invest.* **25**:220.

72. RIGATUSO, J. L., P. G. LEGG, and R. L. WOOD. 1970. Microbody formation in regenerating rat liver. *J. Histochem. Cytochem.* **18**:893.

73. SABATINI, D., K. BENSCH, and R. J. BARRNETT. 1963. Cytochemistry and electron microscopy. The preservation of cellular ultrastructure and enzymatic activity by aldehyde fixation. *J. Cell Biol.* **17**:19.

74. SCOTT, P. J., L. P. VISENTIN, and J. M. ALLEN. 1969. The enzymatic characteristics of peroxisomes of amphibian and avian liver and kidney. *Ann. N. Y. Acad. Sci.* **168**:244.

75. SELIGMAN, A. M., M. J. KARNOVSKY, H. L. WASSERKRUG, and J. S. HANKER. 1968. Nondroplet ultrastructural demonstration of cytochrome oxidase activity with a polymerizing osmiophilic reagent, diaminobenzidine (DAB). *J. Cell Biol.* **38**:1.

76. SHNITKA, T. K., and G. G. TALIBI. 1971. Cytochemical localization by ferricyanide reduction of α-hydroxy acid oxidase activity in peroxisomes of rat kidney. *Histochemie.* **27**:137.

77. SMITH, R. E., and M. G. FARQUHAR. 1965. Preparation of non-frozen sections for electron microscope cytochemistry. *RCA Sci. Instr. News.* **10**:13.

78. STELMASZYŃSKA, T., and J. M. ZGLICZYŃSKI. 1971. Studies on hog intestine mucosa peroxidase. *Eur. J. Biochem.* **19**:56.

79. STRUM, J. M. and M. J. KARNOVSKY. 1970. Ultrastructural localization of peroxidase in submaxillary acinar cells. *J. Ultrastruct. Res.* **31**:323.

80. TSUKADA, H., Y. MOCHIZUKI, and T. KONISHI. 1968. Morphogenesis and development of microbodies of hepatocytes of rats during pre- and postnatal growth. *J. Cell Biol.* **37**: 231.

81. VENKATACHALAM, M. A., M. H. SOLTANI, and H. D. FAHIMI. 1970. Fine structural localization of peroxidase in the epithelium of large intestine of rat. *J. Cell Biol.* **46**:168.

82. VIGIL, E. L. 1970. Cytochemical and develop-

mental changes in microbodies (glyoxysomes) and related organelles of castor bean endosperm. *J. Cell Biol.* **46**:435.

83. WILLIAMS, N. E., and J. H. LUFT. 1968. Use of a nitrogen mustard derivative in fixation for electron microscopy and observations on the ultrastructure of *Tetrahymena*. *J. Ultrastruct. Res.* **25**:271.

84. WOOD, R. L., and P. G. LEGG. 1970. Peroxidase activity in rat liver microbodies after aminotriazole inhibition. *J. Cell Biol.* **45**:576.

85. YAMAMOTO, R. 1966. An electron microscope study of the columnar epithelial cell in the intestine of fresh water teleosts: goldfish (*Carassius auratus*) and rainbow trout (*Salmo irideus*). *Z. Zellforsch. Mikrosk. Anat.* **72**:66.